



Republic of Iraq

Ministry of Higher Education & Scientific Research

University of Kerbala

College of Engineering

Civil Engineering Department

**Enhancement of Flexural Capacity of RC Beams Strengthened
by CFRP Sheets**

A Thesis Submitted to the Council of the Faculty of the College of the
Engineering/University Of Kerbala in Partial Fulfillment of the Requirements for
the Master Degree in Civil Engineering

Written By:

Mohammed Ali Azeez

(B.Sc. in Civil Engineering-2016)

Supervised By:

Asst. Prof. Dr. Jawad Talib Abodi &

Asst. Prof. Dr. Aymen J. Alsaad

(2022 A.D)

(1443 A.H)

بِسْمِ اللَّهِ الرَّحْمَنِ الرَّحِيمِ

يَرْفَعِ اللَّهُ الَّذِينَ آمَنُوا مِنْكُمْ وَالَّذِينَ أُوتُوا

الْعِلْمَ دَرَجَاتٍ

صدق الله العلي العظيم

(المجادلة: من الآية 11)

Examination committee certification

We certify that we have read the thesis entitled "Enhancement of Flexural Capacity of RC Beams Strengthened by CFRP Sheets " and as an examining committee, we examined the student " Mohammed Ali Azeez" in its content and in what is connected with it and that in our opinion it is adequate as a thesis for the degree of Master of Science in Civil Engineering.

Supervisor

Signature:

Name: Asst. Prof. Dr. Jawad Talib Abodi

Date: / / 2022

Supervisor

Signature:

Name: Asst. Prof. Dr. Aymen J. Alsaad

Date: / / 2022

Member

Signature:

Name: Prof. Dr. Sadjad Amir Hemzah

Date: / / 2022

Member

Signature:

Name: Asst. Prof. Dr. Ali Ghanim Abbas

Date: / / 2022

Chairman

Signature:

Name: Prof. Dr. Qasim Mohammed Shakir

Date: 13/11/2022

Signature:

Name: Prof. Dr. Sadjad Amir Hemzah
Head of the Department of Civil Engineering

Date: / / 2022

Signature:

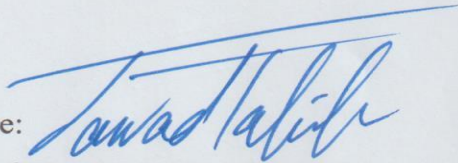
Name: Prof. Dr. Laith Sh. Rasheed
Dean of the Engineering College

Date: / / 2022

Supervisor certificate

We certify that the thesis entitled “**Enhancement of Flexural Capacity of RC Beams Strengthened by CFRP Sheets**” was prepared by **Mohammed Ali Azeez** under our supervision at the Department of Civil Engineering, Faculty of Engineering, University of Kerbala as a partial of fulfilment of the requirements for the Degree of Master of Science in Civil Engineering.

Signature:



Asst. Prof. Dr. Jawad Talib Abodi

Date: / / 2022

Signature:



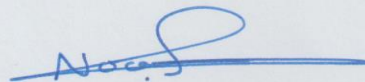
Asst. Prof. Dr. Aymen J. Alsaad

Date: / / 2022

Linguistic certificate

I certify that the thesis entitled " **Enhancement of Flexural Capacity of RC Beams Strengthened by CFRP Sheets** " which has been submitted by **Mohammed Ali Azeez** has been proofread and its language has been amended to meet the English style.

Signature:



Name: **Noor Husam Jaber**

Date: **10/11/2022**

Abstract

Carbon Fiber Reinforced Polymer (CFRP) sheet are used to improve the properties of concrete in structural components such as buildings and bridges. This composite technique is commonly considered wherever high strength-to-weight ratio and stiffness are required. However, one of the significant issues of this system is the delamination problem. At a certain load level, the CFRP sheets start delamination from the concrete substrate, which results in premature failure. As a result, this experimental research aims to control the delamination by using Poly Vinyl Alcohol (PVA) and Steel Fiber (SFRC) with different percentages, arrangements, and techniques. The practical program of the presented study was based on casting (17) reinforced concrete rectangular beams with cross-section dimensions (250 * 150) mm and a length of (2150) mm have been strengthened with CFRP sheets. The one was control beam without PVA or SFRC. The remaining sixteen specimens were divided into two groups. The first group consisted of eight beams that were cast completely with PVA and SFRC materials. The second group comprised another eight beams that were cast with PVA and SFRC from the bottom layer of the beam up to a height of 52 mm. Results showed that utilizing 1.2% of PVA and 1% of steel fiber increased the maximum strength and mid-span deflection for both groups compared to the control beam. Specific values are needed the maximum increase in beam failure load was 54.3% and 47.3%, and the largest increase in the mid-span displacement of the beam was 34.14% and 27.84% for the first and second groups, respectively. The role of the proposed (PVA / SFRC) layer is to control the cracking of concrete and detain or even avoid premature debonding of the strengthening CFRP sheets. Because the (PVA / SFRC) layer's ability to

exhibit strain hardening behavior is primarily determined by the used fiber volumetric ratio, two different steel fiber volumetric ratios (fiber volumetric ratios of 0.5% and 1%, respectively) increased the maximum load in the first and second groups by 10.91% and 8.33%, respectively. Three flexural failure patterns plate-end interfacial debonding, concrete cover separation, and FRP rupture were seen in the tested specimens. The experiments demonstrated that the FRP rupture caused the BSPV 1.0.1.2 specimen to fail.

Undertaking

I certify that research work titled “**Enhancement of Flexural Capacity of RC Beams Strengthened by CFRP Sheets**” is my own work. The work has not been presented elsewhere for assessment. Where material has been used from other sources it has been properly acknowledged / referred.

Signature:

Mohammed Ali Azeez

Date: / / 2022

Dedication

*To
My
Dears
(Family)*

Signature:

Mohammed Ali Azeez

Date: / / 2022

Acknowledgements

Firstly, my great thanks to ALLAH for enabling me to complete my works.

I would like to express my gratitude and thanks to our supervisors, Assist prof. Dr. Jawad Talib Abodi and Assist prof. Dr. Aymen J. Alsaad for their great assistance, guidance and valuable suggestions throughout the research period.

I would also like to thank Assist prof. Dr. Bahaa Hussain for his assistance to me on several occasions during the research period. Thanks also to the head and the staff in the Civil Engineering department, the construction materials laboratory and all those who stood with me to complete this work.

A special thank and gratitude to my family especially My Mother for their care, patience and encouragement throughout the research period.

Finally, I would like to express my extreme love and appreciation to everyone who has supported this work.

Signature:

Mohammed Ali Azeez

Date: / / 2022

Table of Contents

| | |
|--|-------|
| Examination committee certification | I |
| Supervisor certificate..... | II |
| Linguistic certificate..... | III |
| Abstract..... | IV |
| Acknowledgements | VI |
| Table of Contents | IIIIV |
| List of Tables | X |
| List of Figures..... | XI |
| Abbreviations | XIII |
| List of Symbols | XIV |
| Chapter One: Introduction..... | 1 |
| 1.1 General | 2 |
| 1.2 Strengthening. | 3 |
| 1.3 Fiber Reinforcement Polymer (FRP) | 4 |
| 1.4 Delamination Failure of FRP Strengthened Beams | 5 |
| 1.5 High Strength Concrete | 6 |
| 1.6 Research Significance and Objective of the Study | 6 |
| 1.7 Layout of the Thesis | 7 |
| Chapter Two: Literature Review | 9 |
| 2.1 Introduction | 10 |
| 2.2 Delamination CFRP Strengthening Beams | 10 |
| 2.3 Enhancements to Cement-Based Composites..... | 11 |
| 2.3.1 Polymer Modification of Cement Mortars..... | 13 |
| 2.3.2 Hook-Ended Steel Fiber | 14 |

| | |
|--|----|
| 2.4 Properties and Types of Fiber Reinforced Polymer (FRP) | 15 |
| 2.5 Methods of Strengthening Structural Members by FRP..... | 16 |
| 2.5.1 End-Anchorage Systems | 17 |
| 2.5.2 Near Surface Mounted FRP Technique (NSM)..... | 18 |
| 2.5.3 Externally Bonded Reinforced FRP Technique (EBR) | 18 |
| 2.6 Examples of Strengthening Beams by FRP Sheet (EBR)..... | 20 |
| 2.6.1 Kattenbusch Bridge | 20 |
| 2.6.2 The Hata Bridge in Japan &The Foulk Road Bridge..... | 21 |
| 2.6.3 Strengthening Work on The Ibach Bridge in The Year 1991 .. | 22 |
| 2.6.4 Oberriet Rhine Bridge with Externally Bonded CFRP Strips . | 23 |
| 2.7 Researches Related to The De-bonding Mechanism | 25 |
| 2.8 Summary | 27 |
| Chapter Three: Experimental Investigation..... | 28 |
| 3.1 Introduction | 30 |
| 3.2 Mix description | 30 |
| 3.3 Materials | 32 |
| 3.3.1 Cement | 32 |
| 3.3.2 Coarse Aggregate | 33 |
| 3.3.3 Fine Aggregate | 35 |
| 3.3.4 Hook-Ended Steel Fiber | 36 |
| 3.3.5 (PVA)Polyvinyl Alcohol..... | 38 |
| 3.3.6 Reinforcement | 39 |
| 3.3.7 Carbon Fiber Reinforced Polymer (CFRP) Sheet..... | 40 |
| 3.3.8 Epoxy Resin | 41 |
| 3.3.9 Super-plasticizer (SP)..... | 43 |
| 3.4 Concrete Mixes..... | 44 |

| | |
|--|----|
| 3.5 Procedure for Mixing, Preparing and Casting Beams High Strength Concrete | 46 |
| 3.6 Bonding of Composite Materials to Beams | 51 |
| 3.7 Fresh Test and Hardened Testes..... | 54 |
| 3.7.1 Slump Test and Density | 54 |
| 3.7.2 Compressive and Splitting Tensile Strengths | 55 |
| 3.8 Beams Configuration..... | 56 |
| 3.9 Test Procedures and Experimental Setup..... | 58 |
| Chapter Four: Results and Discussion | 60 |
| 1.4 Introduction | 61 |
| 4.2 Fresh Concrete Properties | 61 |
| 4.2.1 Workability (Slump Values), Super-plasticizer (SP) and Density | 61 |
| 4.3 Hardened Concrete Properties..... | 63 |
| 4.3.1 Compressive Strength of SFRC-PVA Concrete | 64 |
| 4.3.2 Splitting Tensile Strength..... | 65 |
| 4.4 Part Two General Behavior of Tested Beams..... | 66 |
| 4.4.1 Beams Cast into one batch (Group 1) | 67 |
| 4.4.2 Beams Cast into Two Batches Group 2 (2YB.RC)..... | 67 |
| 4.5 Effect of Test Parameters | 69 |
| 4.5.1 Studying the effect of parameters for Group One | 69 |
| 4.5.1.1 Effect of Polyvinyl Alcohol Solution on Beams Control | 71 |
| 4.5.1.2 Effect of Hook Steel Fiber on Control Beam..... | 72 |
| 4.5.1.3 Effect of PVA and Steel Fiber (SFRC-PVA) on Control Beam | 73 |
| 4.5.2 Study the effect of parameters on Group Two | 78 |
| 4.5.2.1 Effect of PVA on the Beams that were Cast in Two Batches . | 78 |

| | |
|--|----|
| 4.5.2.2 Effect of an SFRC-PVA on the Beams that were Cast in Two Batches | 85 |
| 4.6 Crack Patterns and Failure Modes | 91 |
| Chapter Five: Conclusions and Recommendations..... | 93 |
| 5.1 Introduction | 96 |
| 5.2 Conclusions | 96 |
| 5.3 Future Work and Suggestions | 97 |
| References | 98 |
| Appendices | 1 |

List of Tables

| | |
|---|----|
| Table 2-1: Mechanical properties of different fibers[30]..... | 16 |
| Table 3-1: Mix Design of the Experimental works..... | 31 |
| Table 3-2: physical properties of the cement used..... | 33 |
| Table 3-3: Chemical composition of the cement [51]..... | 33 |
| Table 3-4: Grading of the coarse aggregate used..... | 33 |
| Table 3-5: The properties of coarse aggregate..... | 35 |
| Table 3-6: Grading of the fine aggregate used..... | 35 |
| Table 3-7: The properties of fine aggregate [51]..... | 36 |
| Table 3-8: Properties of Steel Fiber type Hook Ended CH-65/35..... | 37 |
| Table 3-9: Steel reinforcement properties..... | 40 |
| Table 3-10: Properties of Carbon Fiber Sheets..... | 41 |
| Table 3-11: Properties of Nitowrap Primer and Nitowrap Encapsulation Resin | 43 |
| Table 3-12: Properties of Sika ViscoCrete®-F180G Technical Data..... | 44 |
| Table 3-13: Mix Properties of Concrete used..... | 45 |
| Table 3-14: Description of the Specimens..... | 57 |
| Table 4-1: Concrete properties of all mixes..... | 62 |
| Table 4-2: The average results of compressive strength..... | 65 |
| Table 4-3: Results of the average tensile strength..... | 66 |
| Table 4-4: Results of the tested beams-group 1..... | 67 |
| Table 4-5: Results of the tested beams group 2..... | 68 |

List of Figures

| | |
|---|----|
| Figure 1-1: Strengthening reinforced concrete beam with FRP [3] | 3 |
| Figure 1-2: Type of FRP sheets [7] | 4 |
| Figure 1-3: Delamination failure mechanisms[9]..... | 6 |
| Figure 2-1: Polyvinyl alcohol (PVA)[20]..... | 11 |
| Figure 2 2:Hook Ended steel fiber[27] | 15 |
| Figure 2-3: Stress-Strain Relationships for Different Types of FRP[32].... | 17 |
| Figure 2-4: Glass fiber reinforced polymer (GFRP) Plates at the bottom slab of Kattenbusch Bridge.[43] | 21 |
| Figure 2-5: Repair of pre-stressed box beam bridge girders using tow sheets [30]..... | 22 |
| Figure 2-6: Strengthening work on the Ibach bridge in the year 1991. | 23 |
| Figure 2-7: Bridge over the river Rhine near Oberriet in Switzerland..... | 24 |
| Figure 2-8: Cross-section of the bridge. Figure taken from[31] | 25 |
| Figure 3-1: Geometry of Reinforced Concrete Tested beams..... | 30 |
| Figure 3-2: Flowchart for the specified mix design and beams tested..... | 32 |
| Figure 3-3: Curve for Coarse Aggregate (Gravel) | 33 |
| Figure 3-4: Curve for Fine aggregate (Sand) | 36 |
| Figure 3-5: Hook Ended steel fiber CH-65/35 | 37 |
| Figure 3-6: Polyvinyl alcohol (PVA) | 38 |
| Figure 3-7: Steel reinforcement testing machine | 39 |
| Figure 3-8: (Nitowrap CW CWH 340 GPa) CFRP sheet from Fosroc | 41 |
| Figure 3-9: (a ,b)Hardening and epoxy | 42 |
| Figure 3-10: Sika ViscoCrete® F180G..... | 44 |
| Figure 3-11: The plywood formwork with the reinforcement. | 48 |

| | |
|--|----|
| Figure 3-12: The first group where the model is casted in one batch from the mixer B.RC..... | 49 |
| Figure 3-13: The second group 2YB.RC beam is casted in the form of two batches (2Y) and (250 mm - 2Y)..... | 50 |
| Figure 3-14: CFRP sheet installation stages..... | 52 |
| Figure 3-15: Schematic of CFRP sheet installation stages with | 55 |
| Figure 3-16: Slump test | 55 |
| Figure 3-17: Compressive and Splitting Tensile Strengths..... | 56 |
| Figure 3-18: Flexural testing machine with support and loading details (at Kerbala Construction Laboratory)..... | 59 |
| Figure 3-19: Flexural testing machine with the details of the gauges (at Kerbala Construction Laboratory)..... | 59 |
| Figure 4-1: Mode of Failure of Various Mixtures in Splitting Test..... | 66 |
| Figure 4-2: Failure modes (PVA)concrete | 70 |
| Figure 4-3: PVA load versus deflection -Group1..... | 71 |
| Figure 4-4: Failure modes (SFRC)concrete | 72 |
| Figure 4-5: SFRC load versus deflection -Group 1..... | 73 |
| Figure 4-6: Case 1: SFRC-PVA load versus deflection..... | 74 |
| Figure 4-7: Failure modes (SFRC and PVA) concrete..... | 75 |
| Figure 4-8: SFRC-PVA load versus deflection - Case 2..... | 76 |
| Figure 4-9: Failure modes (SFRC and PVA) concrete..... | 77 |
| Figure 4-10: PVA load versus deflection -Group 2 | 79 |
| Figure 4-12: PVA 2% load versus deflection - compared Group 2 with Group 1 | 81 |
| Figure 4-13: PVA 1.2% load versus deflection - compared Group 2 with Group 1 | 81 |
| Figure 4-14: SFRC load versus deflection -Group 2..... | 82 |

| | |
|---|----|
| Figure 4-15: Failure modes (SFRC)concrete | 83 |
| Figure 4-16: SFRC 1% load versus deflection - compared Group 2 with Group 1 | 84 |
| Figure 4-17: SFRC 0.5% load versus deflection - compared Group 2 with Group 1 | 84 |
| Figure 4-18: load versus deflection (2YBS 0.5% -2Y PV 1.2 , 2.0%) with (CB) | 86 |
| Figure 4-19: load versus deflection (2YBS 1.0% -2Y PV 1.2 , 2.0%) with (CB) | 86 |
| Figure 4-20: The failure of the beams 2YSFRC-2YPVA | 88 |
| Figure 4-21: load versus deflection (2YBS 0.5.1.2 - BSPV 0.5.1.2) with (CB) | 89 |
| Figure 4-22: load versus deflection (2YBS 0.5.2.0 - BSPV 0.5.2.0) with (CB) | 89 |
| Figure 4-23: load versus deflection (2YBS 1.0.2.0- BSPV 1.0.2.0) with (CB) | 90 |
| Figure 4-24: load versus deflection (2YBS 1.0.1.2 - BSPV 1.0.1.2) with (CB) | 90 |
| Figure 4.25: Second group at the final loading stage | 93 |

Abbreviations

| | |
|----------------------------|--|
| CERF | Civil Engineering Research Foundation. |
| RC | Reinforced concrete. |
| FRP | Fiber- reinforced polymer. |
| CFRP | Carbon fiber reinforced polymer. |
| GFRP | Glass fiber reinforced polymer. |
| AFRP | Aramid fiber reinforced polymer. |
| EBR | Externally bonded reinforced. |
| NSM | Near surface mounted. |
| SFRC | Steel Fiber Reinforced Concrete. |
| PVA | Poly vinyl Alcohol. |
| VF | The percentage volume of steel fibers in the concrete mix. |
| ECC | Engineered Cement-based Composites. |
| ACI | American concrete institute. |
| (PVALPVOH or POVAL) | Chemical name PVA mentioned. |
| HK | Type of hook Ended steel fiber. |
| No. | Number. |
| ASTM | American Society for Testing and Material. |
| IQS | Iraqi Specification. |
| kN | Kilo Newton. |
| mm | Millimeter. |
| mg/mol | Molar mass. |
| GPa | Gaga Pascal. |
| MPa | Mega Pascal. |

| | |
|---------------------|--|
| NC | Normal concrete. |
| P/C % | PVA powder as percentage of cement weight. |
| C.A | Coarse aggregate. |
| F.A | Fine aggregate. |
| B.RC | First group beam casted in one batch from the mixer. |
| 2YB.RC | Second group beam is casted in the form of two batches. |
| BSI | Standards Limited, The British Standards Institution. |
| 2Y | Bottom layer deep in the tensile area of RC, whic surrounds the reinforcing steel 52 mm. |
| ORC | Ordinary reinforced concrete. |
| CB | Control Beam. |
| BS 0.5 | Beam with steel fiber 0.5% . |
| BS 1.0 | Beam with steel fiber 1% . |
| BPV 1.2 | Beam with PVA solution 1.2% . |
| BPV 2.0 | Beam with PVA solution 2% . |
| BSPV 0.5.1.2 | Beam with steel fiber 0.5% & PVA solution 1.2% . |
| BSPV 1.0.2.0 | Beam with steel fiber 1% & PVA solution 2% . |
| BSPV 0.5.2.0 | Beam with steel fiber 0.5%& PVA solution 2% . |
| BSPV 1.0.1.2 | Beam with steel fiber 1%& PVA solution 1.2% . |

List of Symbols

| | |
|----------|--|
| A | Cross sectional area of a section (mm ²) |
| A_v | Area of vertical shear reinforcing bar (mm ²) |
| b, b_w | Width of beam (mm) |
| d | Effective Depth (mm) |
| d_b | Diameter of bar (mm) |
| E | Modulus of Elasticity (GPa) |
| f_t | Indirect tensile strength (splitting tensile strength) (MPa) |
| f_{cu} | Cube compressive strength of concrete (MPa) |
| f_y | Yield stress of steel (MPa) |
| h | Total depth of beam (mm) |
| L | Total length of beam (mm) |
| L_n | Clear span of beam (mm) |
| M_u | Ultimate moment capacity (kN.m) |
| M_n | Nominal moment capacity (kN.m) |
| P | Maximum applied load (kN) |
| P_{cr} | Cracking load (kN) |
| P_u | Ultimate load (kN) |
| V_c | Shear strength of concrete (kN) |
| V_s | Shear strength of steel bar (kN) |
| V_u | Ultimate shear strength (kN) |
| V_n | Nominal shear strength (kN) |
| V_f | Volume fraction of steel fibers (%) |
| w/c | Water to Cement ratio |
| ϕ | Size of bar (mm) |

| | |
|------------------|---|
| ρ | Ratio of longitudinal tensile reinforcement |
| ρ_{\min} | Minimum ratio of longitudinal tensile reinforcement |
| $\Delta_{\max.}$ | Maximum deflection (mm) |
| ε | Strain (mm/mm) |

Chapter One: Introduction

Chapter One: Introduction

1.1 General

In recent years, needs a significant portion of North American infrastructure desperately strengthening and rehabilitation. According to research by Civil Engineering Research Foundation (CERF), (1994) the costs associated with replacing and reinforcing all secondary structures are prohibitive. These troubling statistics highlight the importance of developing dependable and cost-effective techniques for repairing and strengthening existing structures. High-tech solutions need to be studied so that new technologies and materials can be used to reconstruct the infrastructure [1]. Fiber-reinforced polymer (FRP) composite system has been established as an efficient method for rehabilitating and reinforcing concrete structures. It is increasingly utilized as an alternative to steel in reinforced concrete structures. Among the various types of FRP materials, CFRP is widely utilized in structural engineering. The externally bonded reinforcement (EBR) has generally been applied through simple installation procedures.

In contrast, external reinforcement of R.C beams with epoxy-bond CFRP has been proven to be an effective tool for increasing bending and/or shear force. This method still has some drawbacks, such as a significant loss of ductility when CRFPs are used in flexure. CFRP delamination problem dominates the failure of R.C beams [2]. Under load, bending/shearing cracks widen and cause high interfacial shear stress, causing the FRP to disband and propagate through the shear span in the direction of the moment.

1.2 Strengthening Beams.

Structural strengthening is the process of upgrading structures before failure improve performance under existing loads or to increase the strength of structural members to carry additional loads. Reinforced concrete structures deteriorate with age and fatigue in the environment. One of several cost-effective engineering solutions is jacketing concrete structures with carbon fabric FRP to reinforce and rehabilitate them. Building rehabilitation refers to restoring a building or structure to a usable state after it has suffered partial damage or failure through repair. Repair is the technical aspect of rehabilitation. It refers to the modification of a structure, partly or wholly which is damaged in appearance or serviceability. There are several methods of strengthening of RC structures using different FRP materials under different schemes including externally bonded FRP (EBR), near surface stabilization reinforcement (NSM) Figure 1-1, end-anchorage systems, FRP jacket, fabric reinforced concrete as well as FRP prestressing techniques to modify existing structures [3].

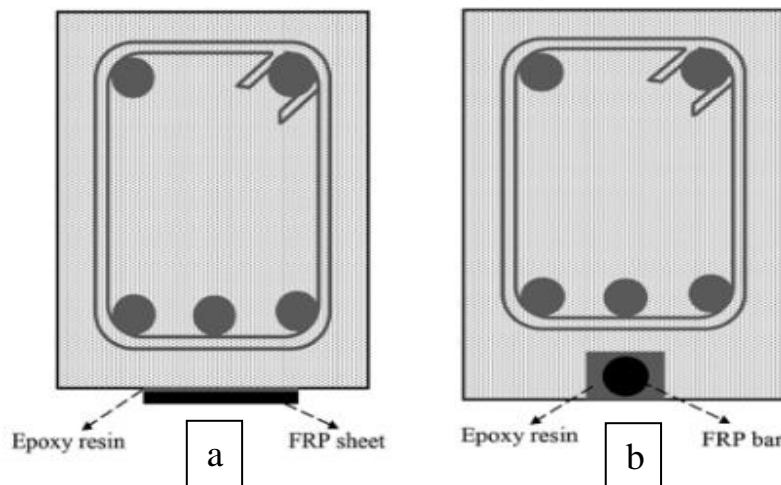


Figure 1-1: Strengthening reinforced concrete beam with FRP [3]

a) Externally bonded reinforcement (EBR), b) Near-surface mounted reinforcement (NSM).

1.3 Fiber Reinforcement Polymer (FRP)

FRP composites were often produced in several forms, such as plates, laminates, and bars. In recent years, CFRP sheet used to repair or strengthen deteriorated structural components, with the polymer resin covering the fibers to hold them together. The benefits of the CFRP include [4]:

- 1- very high strength.
- 2- exceptional fatigue strength.
- 3- corrosion resistance.
- 4- excellent alkaline strength,
- 5- low weight, low thickness, available in any length,
- 6- economical to apply.

The disadvantage FRP is the relatively high material cost compared to steel, however, the total cost of rehabilitation using FRP is about 20% lower than steel due to savings in construction expenses [5].

Carbon fiber reinforced polymer (CFRP), glass fiber reinforced polymer (GFRP), and aramid fiber-reinforced polymer (AFRP) is the most popular fiber composites used in civil engineering applications [6] [7], as shown in Figure 1-2.

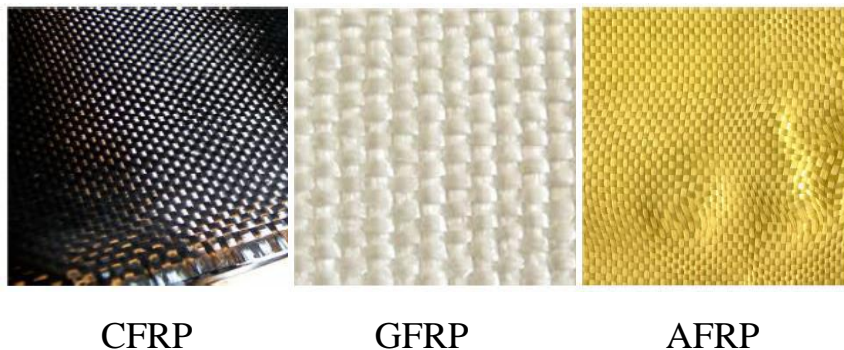


Figure 1-2: Type of FRP sheets [7]

1.4 Delamination Failure of FRP Strengthened Beams

An improperly prepared surface may cause the FRP system to debond before performing the design load transfer. Debonding can occur near the region of the maximum moment due to flexural/shear cracks, or both. The delamination occurs when the interfacial shear and normal stresses exceed the concrete's strength [8], as shown in Figure 1-3 [9]. Various solutions have been proposed to address this issue, from replacing the structure to strengthening various techniques like end-anchorage systems, FRP jacket, and externally bonded reinforcement in grooves (EBRIG). Furthermore, the tensile zone around steel reinforcement was replaced by a cementitious composite material (ECC) [10][11], and the reinforcement Carbon fiber reinforced polymer sheeting (CFRP) was bonded to its bottom surface. This was done to improve the cracking behavior of the reinforced bundles, resulting in improving bonding characteristics. Failure modes can be categorized as follows, according to the ACI Sub-Committee 440 F [12] for investigations of large-scale beams under shear and flexural loads:

- 1- They are crushing the concrete.
- 2- After steel reinforcement yields, FRP ruptures.
- 3- After steel yields, concrete is crushed.
- 4- Delamination of FRP.
- 5- Delamination of the cover.

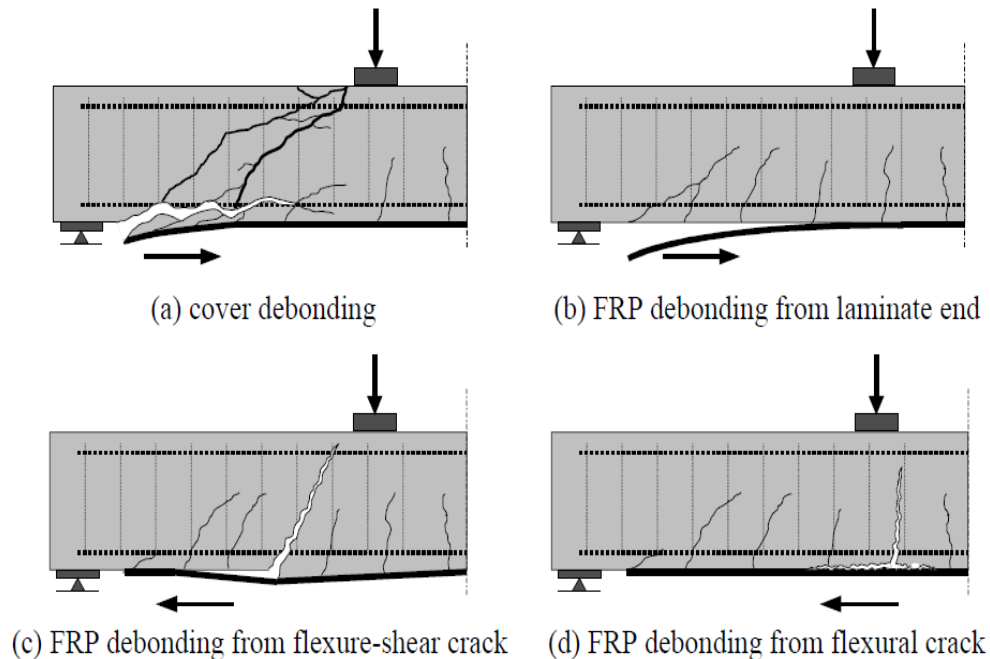


Figure 1-3: Delamination failure mechanisms[9]

1.5 High Strength Concrete

Described as the concrete with good workability, high strength, and long-lasting durability high strength concrete (HSC) has an extensive range of applications in engineering structures. Because of the low water-to-cement (w/c) ratio, HSC is prone to autogenous shrinkage, which increases the risk of early-age cracking. Cracking reduces the load-carrying capacity of HSC structures and allows air, moisture, and other chemical components to enter. Steel fibers and polyacrylamide-based superabsorbent polymers, for example, have been used in HSC to reduce cracking [13].

1.6 Research Significance and Objective of the Study

The main objective of the research program is to reduce the delamination of FRP by modifying the mechanical properties of concrete mix, especially the

tensile strength. Thus, steel fibers and polyvinyl alcohol (PVA) solution were considered to reduce the delamination of FRP carbon fibers in two ways. First, adding a solution of polyvinyl alcohol (PVA) in two percentages (1.2% and 2%) by weight of cement as well as adding two percentages of steel fibers (0.5% and 1%) by volumetric of cement. Then, combining the proportions of the two materials to obtain the best properties of concrete in terms of compressive strength, tensile strength.

The general objectives of this study on the following points:

1. Studying the effect of polyvinyl alcohol (PVA) solution in two weight ratios on the strength of the bond between the beam and CFRP and improving the bending.
2. Study the effect of adding steel fibers (VF) with two volumetric ratios of cement weight on the strength of the bond between the beam and CFRP and improving the flexural in terms of ductility.
3. Studying the effect of percentages ratios of polyvinyl alcohol (PVA) and steel fibers (VF) together and extracting the best mixture ratio to strengthen the bonding area and improving the flexural in terms of ductility.
4. Studying the effect of strengthening a bottom layer region around the reinforcing steel with depth 52 mm (2Y) and comparing it with strengthening the full beam in terms of strengthening the bonding area and the economic situation.

1.7 Layout of the Thesis

The thesis is presented in five chapters:

Chapter One: Provided basic information and a general introduction to FRP, study importance, research objective, problem statement, and method of strengthening using FRP compounds.

Chapter Two: Provided literature review on applications and existing documents dealing with the problem of delamination of carbon fibers by different methods. A literature review on carbon fiber reinforced polymer (FRP) is carried out.

Chapter Three: discussed the current study's materials and test. It also covers the mixing and casting procedures for concrete utilized in the concrete beams and the CFRP installation and testing procedures.

Chapter Four: presented the study's results as well as the measuring indicator considered in this research, such as the final load, deflection, and crack display. Following that, the of this measuring indicator is discussed.

Chapter Five: Illustrated the conclusions drawn from the results obtained in the present study and suggestions for future research and summarizes the study results.

Chapter Two: Literature Review

Chapter Two: Literature Review

2.1 Introduction

Fiber-reinforced polymer (FRP) panels are one of the most promising and effective strengthening technologies for reinforced concrete structures today, and they are used to strengthen and upgrade of structurally inadequate or damaged civilian infrastructure. This technique has several advantages, significantly improving reinforced structures' final behavior, ductility and toughness [14]. These materials are excellent options for use as external reinforcement because of their lightweight, wear resistance and high strength. Exterior-bonded FRP sheets were used to increase the bending elements' torque capacity and improve containment in the compression element [15]. This chapter examines the available data and research on approaches for reducing CFRP reinforcing beam delamination. The review also includes previous studies of steel fiber and vinyl alcohol solution (PVA) used in RC. The literature review also included a summary of previous CFRP External Beam Enhancement Technology (EBR) carbon studies.

2.2 Delamination CFRP Strengthening Beams

This chapter explains the major research goal of removing FRP from concrete beams and gives the necessary knowledge for designers to build FRP-reinforced concrete beams. According to studies, FRP-linked composites can be utilized externally to increase structural element performance, such as bearing capacity, stiffness, ductility, performance loading, fatigue, and environmental durability. A significant concern regarding the efficacy and safety of this method is the potential for brittle failures. Unless adequately considered in the design process, such failures

may significantly reduce the reinforcement's effectiveness. In recent years, many researchers have focused on this important issue through experimental and theoretical modelling investigations that failed to correct the failure of FRP-reinforced concrete (RC) [16][17][18].

2.3 Enhancements to Cement-Based Composites

Engineered Cement-based Composites (ECC) are a type of Fiber Reinforced Concrete (FRC) that includes the components of ordinary concrete, such as cement and cement extenders, aggregates, water, and additives for workability adjustments. Polymer fibers in low volume percentages (up to 2%) are added to the carefully mixed components to complete the response [19]. One of the most important applications of PVA is in the construction industry. This PVA could be used as a fiber enhancer in cement-based composite materials and a pre-curing agent to modify surface aggregate [20]. In this type of composite material, the interaction of cement and polymer results in a microstructure with distinct characteristics [21]. Chemically bonded ceramics are another name for this composite. The role of polymers in composite materials such as cement mortar is divided into three major functions:

1. It performs as a result of rheological agents acting as coverings on separate cement particles, reducing inter particle role.

2. Particle packing as a filler in spaces between unreacted grains of cement and polymers react chemically by cement hydration products to arrange an essential microstructural product, such as the bury phase areas [22].

3. Water-soluble polymers and polymers for aqueous dispersal are frequently used to improve the properties of concrete mortar and cement-based composites [23].

large air voids form when the cement and polymer admixture are combined. The mixing method was investigated to understand the mechanism of air voids formation better. The procedure includes pre-wetting the cement and sand with pure water before adding the PVA solution or dispersal [23], as shown in Figure 2-1.

ECC's behavior depends on the fiber crack-bridging law and the degree of heterogeneity in the material. Crack initiation sites are typically at material flaws, which in most cases are bubbles of entrapped air (voids). Crack initiation behavior is therefore influenced by the size and spatial distribution of voids in the material [24]. Brittle failure is the most common failure caused by premature FRP delamination and concrete cover separation [25].

J.F. Chen *, **J.G. Teng** [25], investigated the main shear failure modes identified for shear-strengthened RC beams with externally bonded FRP reinforcement. they wanted to create a new design proposal for FRP-strengthened RC beams that fail in shear due to FRP debonding. First, a review of existing research was presented, which identified the shortcomings of all existing approaches. A new shear strength model for debonding failures in FRP shear strengthened RC beams was then developed based on a rational bond strength model between FRP and concrete. Based on a thorough review, the new model was found to compare favorably with experimental data collected from the literature. Finally, a design proposal that can be used in practical design was presented.

2.3.1 Polymer Modification of Cement Mortars

Polyvinyl alcohol (PVA) has been used in many general applications for approximately 90 years as an initial artificial colloidal [20]. One of the most important applications of PVA is in the construction industry. This PVA could be used as a fiber enhancer in cement-based composite materials and a pre-curing agent to modify surface aggregate. Its chemical name refers to PVA as (PVAL PVOH or POVAL) [20]. PVA is primarily made by polymerizing vinyl acetate as a monomer into (PVAc), which is then shadowed by hydrolysis of the PVAc group to PVA [26]. Commercial grade PVA is usually classified into two types (based on their degree of polymerization and hydrolysis), namely (a) fully hydrolyzed group with more than 98% mole of acetate groups replaced by alcohol groups and (b) partially hydrolyzed group with 87-89% mole of acetate groups replaced by alcohol groups. Fully hydrolyzed grade PVA is soluble in hot water and has good film-forming characteristics (film formed is insoluble in water at lower temperatures) and good adhesive properties, as indicated in Figure 2-1. PVA adhesive can be converted to water-resistant products by cross-linking its linear chains with formaldehyde boric acid, salts and other insolubility agents [20].



A) PVA Powder

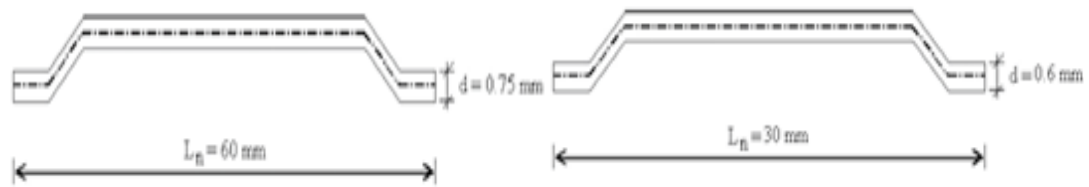


B) PVA After completely dissolved.

Figure 2-1: Polyvinyl alcohol (PVA)[20].

2.3.2 Hook-Ended Steel Fiber

Steel Fiber Reinforced Concrete (SFRC) is a composite material of cement, fine and coarse aggregates, and discrete, discontinuous steel fibers. Only after the steel fiber has failed or been removed from the concrete fail under stress. The SFRC has many excellent dynamic performances such as high resistance to explosion and penetration compared to traditional concrete. The ability of SFRC to transfer stresses across a cracked section increases the toughness of concrete in the hardened state, which is one of its most important properties. Steel fibers are the most widely used of the various types of fibers currently available. Significant research has been conducted to evaluate the mechanical properties of fiber-reinforced cement composites, such as tensile, compressive, bending, and impact strength. Fiber type, appearance ratio, fiber density fraction, and aggregate size all impact the mechanical properties of SFRC. This section also attempted to determine the effect of fiber addition and investigate its impact on concrete behaviour and strength[27] [28] [29] in Figure 2-2.



Hook Ended steel fiber HK-50/30

Hook Ended steel fiber HK-80/60

Figure 2-2: Hook Ended steel fiber [27]

2.4 Properties and Types of Fiber Reinforced Polymer (FRP)

The term "composite" refers to any combination of two or more distinct materials that are shared an interfaced. The term "composite" is used in this work to describe a limited assembly of materials with a polymer matrix reinforced with continuous fibers.

The continuous fiber classifications such as glass, aramid, and carbon as common reinforcements for FRP reinforcement systems. Table 2-1 displays typical fiber properties.

a- The material carbon fiber (CFRP): Carbon fibers are made from precursors of polyacrylonitrile (PAN), pitch, or rayon fibers. A "tow," which is a bundle of unbroken carbon filaments, is the basic element of carbon fiber.

b- The glass fiber (GFRP): Glass fibers are silica-based glass compounds that can be modified to produce various qualities by including metallic oxides. Structural glass, or S-glass, has strong corrosion resistance.

c-Fiber Aramid (AFRP): Aramid fiber is an aromatic Polyimide with high tensile strength and flexibility. Aramid fibers are useful in high-stress and vibration-prone structural voids but are more expensive than other fibers[6][7].

Table 2-1: Mechanical properties of different fibers[30]

| Fiber Types | | Density ρ [g/cm ³] | Modulus of Elasticity E [GPa] | Tensile Strength ft [MPa] | Extension% |
|-------------|---------------|--|-------------------------------------|---------------------------------|------------|
| Glass | E-glass | 2.6 | 72 | 1.72 | 2.4 |
| | S-glass | 2.5 | 87 | 2.53 | 2.9 |
| Carbon | High strength | 1.8 | 230 | 2.48 | 11 |
| | High modulus | 1.9 | 370 | 1.79 | 0.5 |
| Aramid | Kevlar 29 | 1.44 | 100 | 2.27 | 2.8 |
| | Kevlar 49 | 1.44 | 125 | 2.27 | 1.8 |

The CFRP is used in approximately 95% of civil enhancement applications [31].

2.5 Methods of Strengthening Structural Members by FRP

The structural elements of the R.C can be strengthened by attaching the FRP to the concrete surface. Most reinforced members, however, suffer from a failure to correct the FRP concrete interface. The most common structural reinforcement technologies are External Enhanced FRP (EBR), Near Surface Stabilization Technology (NSM), and Mechanically Stabilized FRP Reinforcement (MF-FRP).

The following sections describe the FRP techniques used to reinforce the structural elements used in the research program (EBR). The mechanical properties and chemical compounds of these fibers have been distinguished, and a comparison of these types of FRP composites with steel reinforcing bars and steel tendons in terms of stress-strain relationships is shown schematically in Figure 2-3 [7][32].

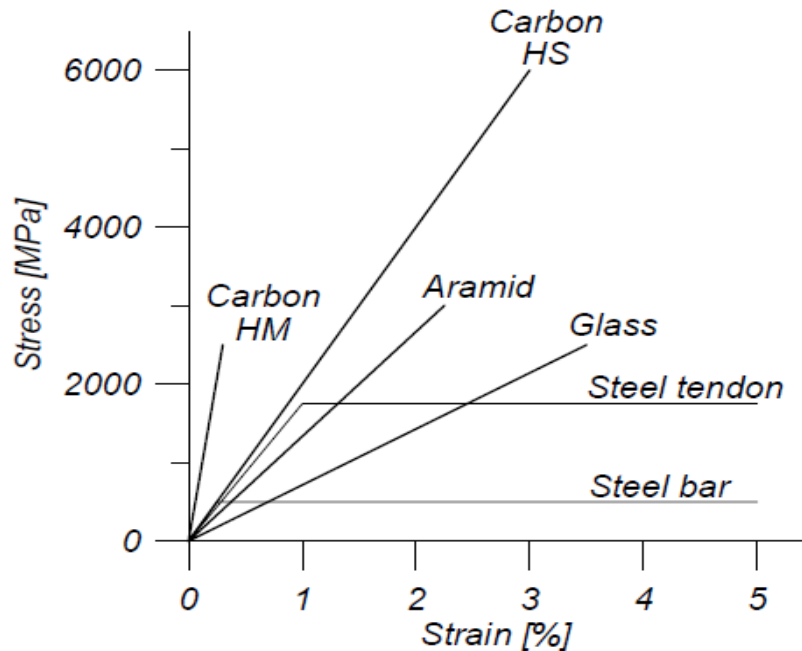


Figure 2-3: Stress-Strain Relationships for Different Types of FRP[32]

2.5.1 End-Anchorage Systems

End anchoring is one of the most important factors when retrofitting reinforced concrete beams with CFRP strips. The bearing capacity of the beam and the failure characteristics of the CFRP are affected by the performance of the anchor systems. Many researchers have investigated the final anchorage technique[33][34].

Clamps, stirrups, U-shaped casings, and anchorage bolts near the end of the FRP have all been used to prevent delamination[35][36].

Ahmed Khalifa, Antonio Nanni [36], Investigated was the shear performance of T-section RC beams with shear deficiencies that were reinforced with various configurations of CFRP sheets. According to the test results, the externally bonded CFRP reinforcement can be used to increase the beams' shear capacity. Increase in shear strength of 35–145% was achieved, and if

adequate anchoring is provided, the performance of CFRP that is externally bonded can be significantly improved. This study looked at wrapping patterns, the amount of CFRP, the combination of 90° and 0° plies, and CFRP end anchorage. The U-wrap with end anchorage was the most effective configuration, according to the results as well. The shear capacity was significantly increased thanks to the use of U-anchors. Additionally, at the very end, the failure mode switched from CFRP debonding to an exural failure mode.

2.5.2 Near Surface Mounted FRP Technique (NSM)

The NSM method is based on bonding the CFRP laminate or rods into small open grooves in the concrete cover of the to-be-strengthened element [37]. Many researchers have used NSM as a promising technique to increase concrete elements' bending and shearing strength [38]. Near the surface FRP Technique (NSM) drawbacks are; the bar cover is thick enough for grooves of a desirable size to be housed[39], and the available knowledge of the FRP method of NSM is much more limited than of the FRP method of external sureties, as reflected in the absence of relevant provisions in the existing guidelines on reinforcing the FRP of published concrete structures by[8].

2.5.3 Externally Bonded Reinforced FRP Technique (EBR)

Externally bonded reinforcement (EBR) with CFRP is the most commonly used technique for strengthening and modernizing R.C structures. Recently, there has been a significant increase in the use of this technique[40].

The steps listed below are the most commonly used in practice for strengthening work using the EBR technique.

- Sandblasting or grinding can be used to prepare the concrete surface.

- Clear the concrete surface from dust and other impurities with an air compressor.
- The primer is sprayed onto the concrete surface and left to dry. Some laminates do not need to be primed at all.
- The epoxy is applied to the concrete surface, followed by the installation of the fabrics, and the process is repeated if additional layers are required. The air voids in the adhesive layer are removed with a roller, and the material is straightened.
- Moreover, epoxy is applied to the laminate surface prior to the installation of the laminate to strengthen the bonding of the laminate plate. Remove any air voids and ensure that the epoxy is distributed evenly [32] [41] [42].

A. Hosny, H. Shaheen, A. Abdelrahman, and T. Elafandy, [39] studied the application of three-way GFRP strips (0°, 90°, 45°) connected to the lower chord and the sides of the samples on two layers with different orientations. The program consists of a total of twelve T-beams with overall dimensions of 460 * 300 * 3250 mm. The beams were tested under cyclic loading until failure to examine the bending behavior. Different reinforcement ratios, fiber directions, locations and assemblies of CFRP and GFRP segments were attached to the beams to determine the best reinforcement scheme. Various proportions of steel reinforcement were also used. Adoption of an analytical model based on the stress-strain properties of concrete, steel and FRP. The maximum measured stress in the rebar was 2.8% for the control sample, while it ranged from 1.0% to 1.5% for the reinforcement. This indicates that when the concrete beams fail, the stress in the rebar is lower in the reinforced samples than in the control sample.

2.6 Examples of Strengthening Beams by FRP Sheet (EBR)

The reinforcement of concrete girders with FRP has become increasingly popular as this method improves the bending resistance of the beams. Because many concrete girders in bridges can have a small concrete cladding, rehabilitation of reinforced concrete bridges has recently become a significant issue. The high-strength lightweight ratio is the weather resistance and the main benefits (FRP). This technique was developed at the Swiss Federal Laboratory for Materials Testing and Research in 1980. Many researchers have investigated the flexing and shearing of concrete beams (FRP) [10]. The following section summarizes some global research and focuses primarily on the Usage Reinforcement Method (FRP) on the behavior of externally bound surface configurations of concrete girders under flexural load. Numerous bridges use this method, but this section will provide chronological examples of some of these bridges.

2.6.1 Kattenbusch Bridge

The Kattenbusch bridge in Germany was the first in the world to use EBR Glass Fiber reinforcement polymers (GFRP). This is a multi-span box girder bridge constructed in situ. The working joints are located at the counter-flexion points where the tendons connect. Cracks were discovered at these work joints on the Kattenbusch Bridge in the 1980s. The durability of the lower slab reinforcement and tendons was no longer guaranteed due to increased fatigue stresses. Prof. Ferdinand S. Rostásy advised building authorities to utilize the EBR strengthening technique with GFRP plates.

These plates were caused by the low modulus of elasticity of the relatively thick GFRP (Figure 2-4). The building authorities heeded the advice, and to the authors' knowledge, the GFRP plates are still in use[43].



Figure 2-4: Glass fiber reinforced polymer (GFRP) Plates at the bottom slab of Kattenbusch Bridge.[43]

2.6.2 The Hata Bridge in Japan &The Foulk Road Bridge

Retrofit applications with FRP composites increased significantly after the early 1990s, including the GFRP towing sheets utilized on the Hata Bridge in Japan to increase transverse bending capacity, as shown in Figure 2-5, carbon tow sheets were utilized on the Foulk Road Bridge in Delaware to prevent transverse cracking in the pre-stressed beams [30].

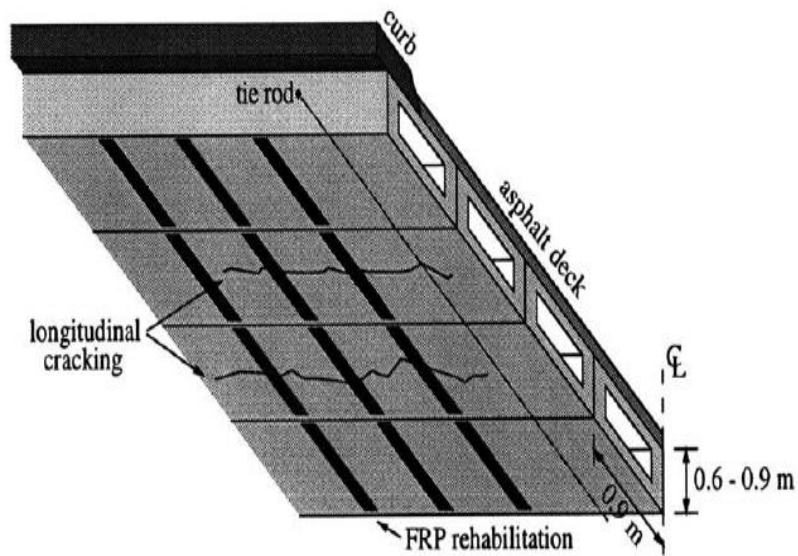


Figure 2-5: Repair of pre-stressed box beam bridge girders using tow sheets [30].

2.6.3 Strengthening Work on The Ibach Bridge in The Year 1991

In 1991, the Ibach Bridge near Lucerne, Switzerland, was reinforced successfully with CFRP bands, see Figure 2-6. While installing new traffic lights on the bridge, a pre-stress tendon in the external web was accidentally damaged, and an oxygen lance completely severed several of its threads. Thus, the bridge was repaired using three CFRP laminates, two of which had dimensions of 150 mm 5000 mm 1.75 mm and the other of which had dimensions of 150 mm 5000 mm 2 mm[44]. The fiber content was 55% (Vol%), and the elastic modulus was 129 GPa.



Figure 2-6: Strengthening work on the Ibach bridge in the year 1991.

2.6.4 Oberriet Rhine Bridge with Externally Bonded CFRP Strips

Another project that was completed only a few years later is described below, and due to the ease of access, a monitoring campaign was possible. Built in 1963, the Rhine Bridge connects Oberriet, Switzerland, to Meiningen, Austria, and spans the Rhine in three continuous spans. 2-7 diagram. The steel-concrete composite superstructure is depicted in Figure 2-8. CFRP tapes with a 12 cm width and a length of 4.2 m from Sika Corporation (Zurich, Switzerland) were applied to the bottom of the slab to reinforce the joyous bending moment in the bridge's cross-section. 670-meter strips were used in total. Walser et al. described the design of the reinforcing project [45]. Bänziger & Köppel & Partner de Buchs in Switzerland was the project engineer.



Figure 2-7: Bridge over the river Rhine near Oberriet in Switzerland

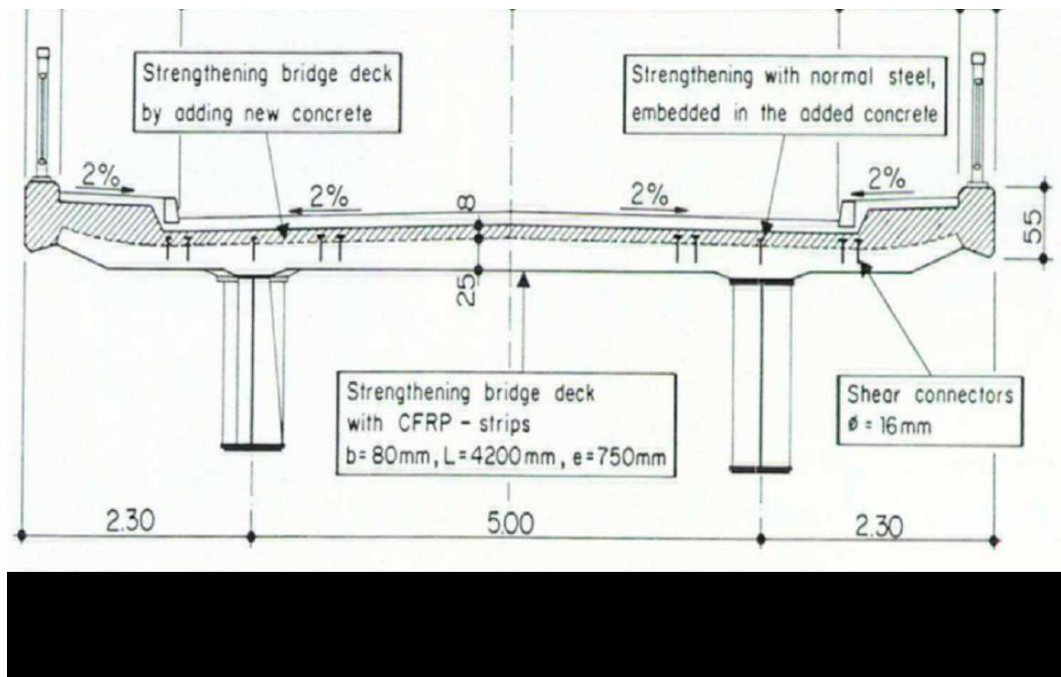


Figure 2-8: Cross-section of the bridge. Figure taken from [31]

2.7 Researches Related to The De-bonding Mechanism

J. Yin, Z.S. Wu* [46]: Beam dimensions (90 length* 15 high * 10 width) cm reinforced with FRP, 70 cm in length. In all cases, the original crack always occurred near the middle of the span. As the steel fiber volume increased, the newly formed cracks tended to be distributed. The ultimate failure mode changed from peeling-induced debonding, as observed in the cases of steel fiber percentage 0.25 and steel fiber percentage 0.50, to the FRP sheet failure in the case of steel fiber percentage 1.00. The micro-cracks in concrete near the connecting interface first occurred concerning the fracture girders. The ultimate failure mode also changes from peeling-induced bonding to FRP rupture when the steel fiber ratio is increased to 1% which reduces the crack effect on the bonding area, so the FRP sheet can sufficiently exert its strengthening effect.

H. Afefy, N. Kassem, and M. Hussein.[10], Tested six beams of dimensions (220 length * 30 height * 15 width) cm and replacing the steel tensioning area bottom layer (depth 2Y) from the engineering cement compounds (ECC) with three different proportions of polypropylene fibers (0.5%, 1% and 1.5% fiber volume ratio).The experimental results showed that the used CFRP reinforcing plate increased the ultimate load by about 28.8% compared to the control beam unreinforced with carbon fiber, and this increase reached about 48.5% by applying the same CFRP sheet to the proposed ECC transition layer with a 1.5% fiber volumetric ratio. The combined effect of the ECC transition layer and the EB-CFRP sheets showed a greater delay in crack appearance.

M.Esfahania, M. Kianoush (2007)[47]. The bending strength of R.C beams reinforced with a CFRP sheet was investigated. The steel reinforcement ratio,

as well as the length, width, and number of CFRP layers, were the experimental variables. There were twelve R.C beams and three different steel reinforcing ratios used. The tested beams were 150mm wide, 2000mm long, and 200mm high. Three control beams were tested, and nine reinforced CFRP laminates were installed. The bending strength of the R.C beams reinforced EBR CFRP laminates increased compared to the control beams. The experimental results revealed that when using a small steel reinforcing ratio compared to the maximum steel reinforcing ratio specified in these two guides, the increased bending resistance calculated using ACI.440-2r-02 and ISIS Canada models is overstated.

Elena Benvenuti^{1*}, Nicola Orlando^{1*}. [48] (2017), studied a practical computational framework based on the regulated the eXtended Finite Element Method (XFEM) . The objective was to predict the structural behaviour of SFRC beams strengthened with FRP plates subjected to bending tests. The pillars of the proposed process included : (i) adopting a regularized kinematics governed by a regularization length related to the bridging effect exerted by steel fibers; (ii) an appropriate variation formula where the stress superposition does not hold, (iii) a definition based on the mechanism of the detachment surface level assembly based on the mode of experientially observed detachment in the experiments.

The main conclusion of this study is that the entire structural trajectory, from early cracking to final FRP detachment, was perfectly consistent with the experimental reference results.

Najm. H, A.Naaman, T-J.Chu, and R. E. Robertson,[49][50]: The effects of adding polyvinyl alcohol (PVA) to a cement matrix to improve binding of the fiber-matrix interface are described in two parts of this article. Steel and brass fibers were used, respectively. (Simulating brass-coated steel fibers) in

a series of shrinkage tests, the load relative to the overall slip has been recorded until full shrinkage.

The slats were measured from the point where the fiber penetrated the layer. The first article discusses the mechanical effects of adding PVA, while the second examines microscopic observations. Part 2 discusses the correlation between the two studies and concludes. It is expressly noted that adding PVA in the amount of 1.4% by weight of the cement improved bond strength and friction resistance significantly during the extraction work after the peak load.

2.8 Summary

1- When FRP is used to strengthen a R.C beam, its flexural resistance increases, and the deflection decreases.

2- When the CFRP sheet is used as an external reinforcing strengthening, it has a sign on the ultimate load, crack pattern, deviations and other factors, as follows:

- i) It increases the capacity and ultimate load of the beams.
- ii) The crack development is delayed, and the crack width is reduced.

3- Externally bonded reinforcing technique (EBR) reinforcement proved useful in terms of the structural behavior of beams under loads.

4- SFRC is a composite material made of cement, fine and coarse aggregate, and separated steel fibers in proportions ranging from 0% to 3% by volume of cement. When using FRP-reinforced beams, the crack widths were reduced[27][28].

5- The cement and polymers (PVA) mixture results in a significant air gap. The mixing method was studied in order to study the creation of voids. The process consisted of pre-wetting cement with sand, cement, and pure water before adding PVA solution[23].

6- The strength of the FRP-reinforced beams decreases when delamination initiates and propagates the beam failure around the shear and flexure cracks caused by stress concentrations in these areas. It is avoidable by lowering the stress level in the adhesion layer. The delamination occurs when the surface shear and normal stresses exceed the concrete's resistance. Due to the concentration of stresses in these zones, the failure of the beam propagates around the shear and bending cracks. This can be avoided by reducing the pressure on the adhesion layer. To address the issue, this research will concentrate on concrete beams under flexion load and reinforced with carbon fiber reinforced polymer (EBR-CFRP) optimization of the steel tensile area.

Chapter Three: Experimental Investigation

Chapter Three: Experimental Investigation

3.1 Introduction

This chapter aims to present cast experimental specimens that cover some applications and get results to be the reference for comparing. The experimental investigation was carried out in the structural laboratory of the Civil Engineering Department at the University of Kerbala. The experimental work consisted of flexural tests on seventeen samples of reinforced concrete beams. Furthermore, the characteristics of the materials utilized in this laboratory study, the specifics of the casting specimens, the test procedure, and the needed instruments are all explained. The details configuration of the beams can be seen in Figure 3-1. The experimental work is described in the following parts.

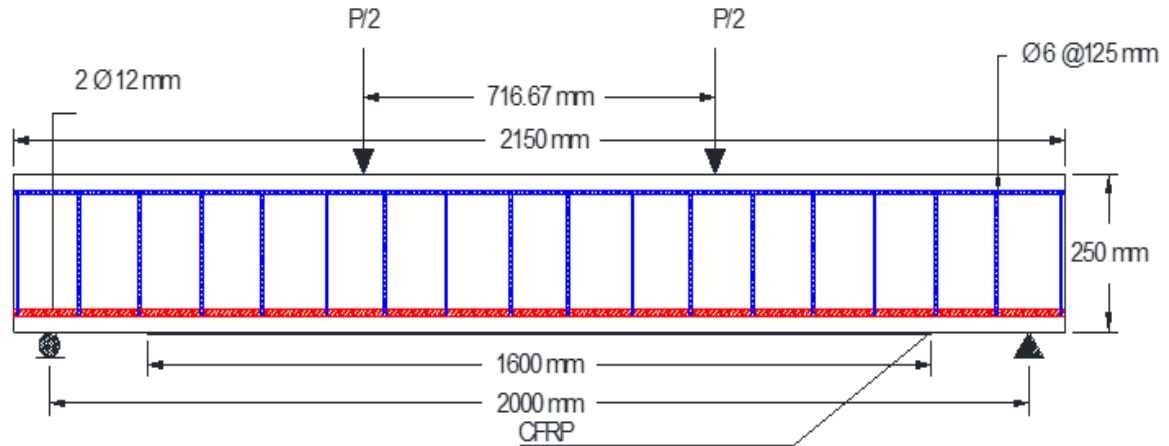


Figure 3-1: Geometry of Reinforced Concrete Tested beams

3.2 Mix description

Nine different types of structural concrete mixes have been designed based on some trial's mixes. All mixes were tested in fresh property state

(Density and workability) and hardened properties (compression, splitting tensile).

Some trials were conducted to determine the effect of steel fibers and polyvinyl alcohol solution (PVA) on various concrete properties and their applicability in the construction field and reduce delamination between concrete beams and carbon fiber CFRP. The first reference mix (N.C) with a compression resistance (f_c') of (30 MPa) was chosen to achieve this compression strength target. The second and third mixtures used steel fibers as a percentage of cement volume, VF 0.5%, VF 1%, Fourth, and fifth mixtures used PVA powder as a percentage of cement weight. Using as solution P/C (P/C 1.2%, P/C 2%) then combined the proportions of the two materials to obtain the best properties of concrete in terms of compressive strength and tensile strength and improve workability with super-plasticizers. The experimental work is described in the following parts and includes the beams tested, as indicated in Figure 3-2. As a result, nine mixed designs will be examined, as indicated in Table 3-1.

Table 3-1: Mix Design of the Experimental works

| No. of Mixes | Features of Mix Design | Name of Mixtures |
|--------------|---|------------------|
| 1 | Normal concrete (control mixture) | N.C |
| 2 | steel fiber 0.5% | VF 0.5 |
| 3 | steel fiber 1% | VF 1 |
| 4 | (P/C) PVA solution 1.2% | PV 1.2 |
| 5 | (P/C) PVA solution 2% | PV 2 |
| 6 | steel fiber 0.5% &(P/C) PVA solution 1.2% | VFPV 0.5.1.2 |
| 7 | steel fiber 1% &(P/C) PVA solution 2% | VFPV 1.0.2.0 |
| 8 | steel fiber 0.5%&(P/C) PVA solution 2% | VFPV 0.5.2.0 |
| 9 | steel fiber 1%&(P/C) PVA solution 1.2% | VFPV 1.0.1.2 |

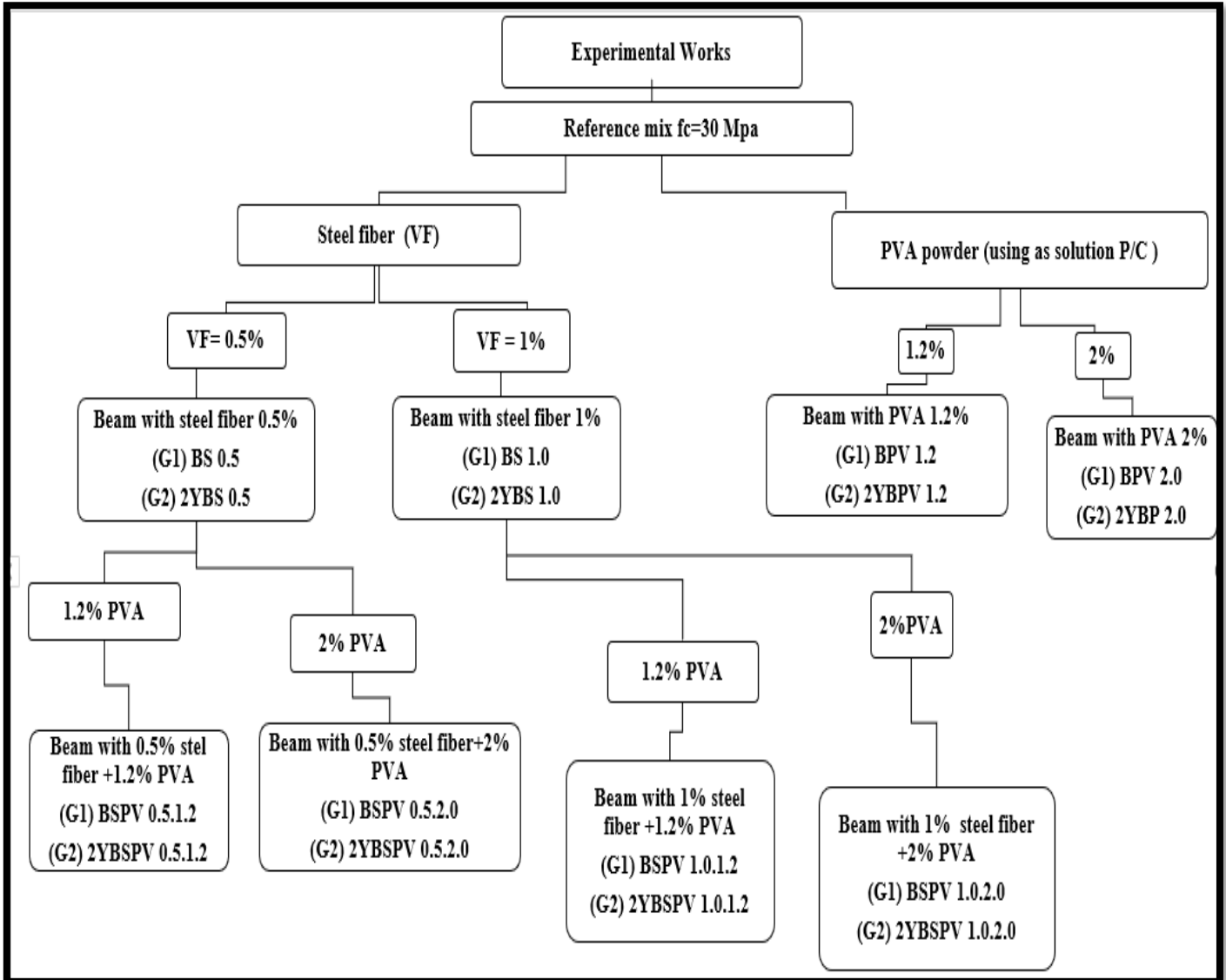


Figure 3-2: Flowchart for the specified mix design and beams tested

3.3 Materials

3.3.1 Cement

The cement utilized in all experimental programs is Type I Portland cement that satisfies the Iraqi specification (IQS No. 5/1984) [51]. Tables 3-2 and 3-3 indicate this type of cement's physical properties and chemical compositions, respectively. These tests were carried out in the structural laboratory of the College of Civil Engineering, University of Kerbala.

Table 3-2: physical properties of the cement used

| Physical properties | Result | Limit of (IQS. No. 5/1984) |
|--|--------|----------------------------|
| Compressive strength (MPa) Three days | 18.3 | ≥ 15 |
| Seven days | 25 | ≥ 23 |
| Setting time (vicats method) | | |
| Initial setting (min) | 2:42 | ≤ 45 |
| Final setting (hr) | 3:44 | ≤ 10 |
| Soundness (expansion), mm | 0.53 | ≤ 10 |
| Specific surface area method (Blaine method) (m^2/kg) | 332 | ≥ 300 |

Table 3-3: Chemical composition of the cement [51]

| Composition of oxides | Abbreviation | % By weight | Limit of (IQS. No. 5/1984) |
|------------------------|-------------------------|-------------|----------------------------|
| Alumina | Al_2O_3 | 4.11 | - |
| Silica | SiO_2 | 21 | - |
| Lime | CaO | 60 | - |
| Iron oxide | Fe_2O_3 | 5.5 | - |
| Lime saturation factor | F.L. S | 0.85 | 0.66-1.02 |
| Magnesia | MgO | 3 | $\leq 5\%$ |
| Loss on Ignition | L.O. I | 3.3 | $\leq 4\%$ |
| Sulfate | SO_3 | 2.2 | $\leq 2.8\%$ |
| Insoluble residue | I.R | 0.4 | ≤ 1.5 |

3.3.2 Coarse Aggregate

The coarse aggregate used is pre-graded gravel with a maximum size of 10 mm, which was taken from the (Al-Akhaidher) region. The gravel was washed to eliminate dust before being dried in the air to obtain a saturated

surface for each batch. The sieve analysis and grading curve for gravels are shown in Table 3-4 and Figure 3-3, which are by American standards (ASTM C33/2003) [52]. Table 3-5 shows how the physical parameters matched the Iraqi standard (IQS. No. 45/1984) [53]. All these tests were done in the structural laboratory of the College of Civil Engineering, University of Kerbala.

Table 3-4: Grading of the coarse aggregate used

| Sieve size (mm) | Limits ASTM C33/2003 | | Percentage passing of coarse aggregate (Coarse. Aggregate) |
|--------------------|----------------------|------------|--|
| | Min. Limit | Max. Limit | |
| 1.18 | 0 | 5 | 0 |
| 2.36 | 0 | 10 | 4 |
| 4.75 | 10 | 30 | 16 |
| 9.5 | 85 | 100 | 95 |
| 12.5 | 100 | 100 | 100 |

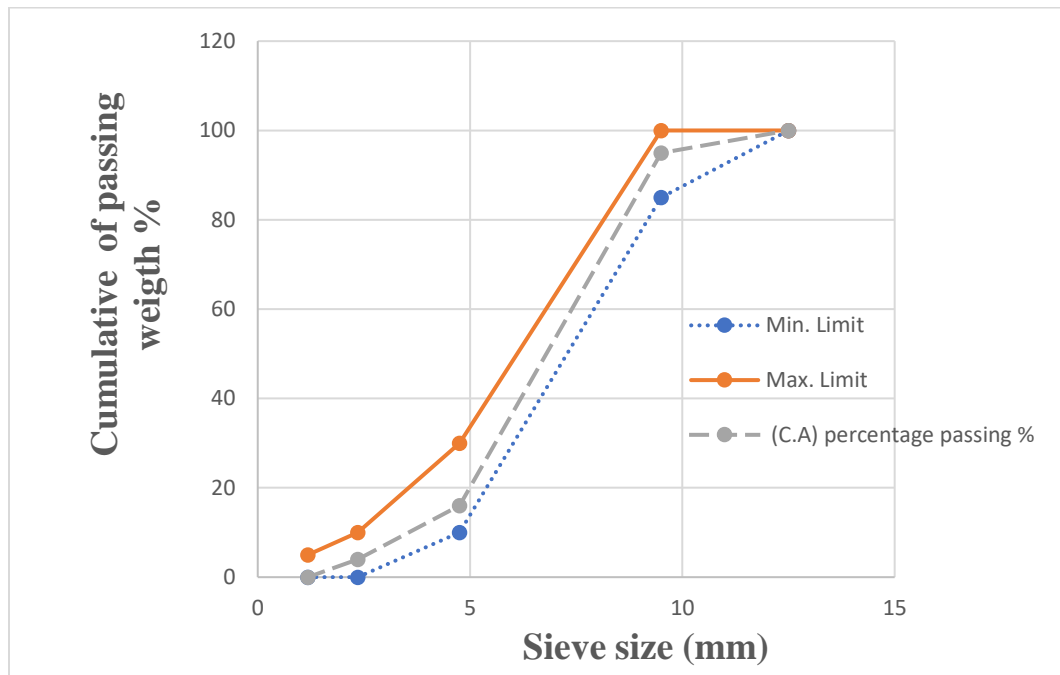


Figure 3-3: Curve for Coarse Aggregate (Gravel)

Table 3-5: The properties of coarse aggregate

| Characteristics | Test results | Limits of (IQS. No. 45/1984) |
|--------------------------------------|--------------|------------------------------|
| Maximum size (mm) | 10 | (5 - 10) |
| Material finer than 75 μm | 0.3 | 3% (max.) |
| Sulfate content (SO ₃) % | 0.062 | 0.1% (max.) |
| Specific gravity | 2.5 | - |
| Absorption % | 0.51 | - |

3.3.3 Fine Aggregate

Natural sand (Al-Akhaidher) with a maximum size of 4.75 mm was used in the experimental program. Sand was used after it was dried. Table 3-6 and Figure 3-4 show the sieve analysis of fine aggregate (sand) and the grading curve according to Iraqi Standards (IQS. No. 45/1984) [53]. Table 3-7 displays the physical properties based on the same specification. These tests were done in the structural laboratory of the University of Kerbala.

Table 3-6: Grading of the fine aggregate used

| Sieve size (mm) | Limits of (IQS. No. 45/1984) (zone 2) | | (Fine. Aggregate) Percentage passing of fine aggregate % |
|--------------------|---------------------------------------|------------|--|
| | Min. Limit | Max. Limit | |
| 0.15 | 0 | 10 | 0 |
| 0.3 | 8 | 30 | 12 |
| 0.6 | 35 | 59 | 45 |
| 1.18 | 55 | 90 | 65 |
| 2.36 | 75 | 100 | 80 |
| 4.75 | 90 | 100 | 90 |
| 9.5 | 100 | 100 | 100 |

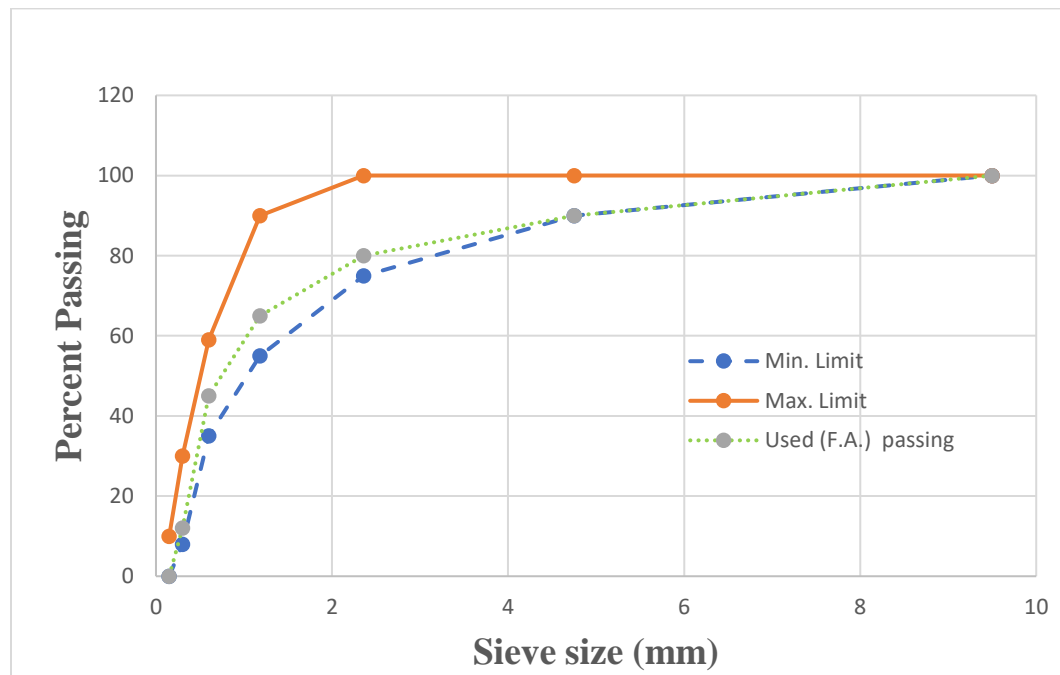


Figure 3-4: Curve for Fine aggregate (Sand)

Table 3-7: The properties of fine aggregate [51]

| Characteristics | Results | Limit of (IQS. No. 45/1984) |
|--------------------------------------|---------|-----------------------------|
| Material finer than 75 μm | 2.1 | 5% (max.) |
| Sulfate content (SO_3) % | 0.1 | 0.5% (max.) |
| Specific gravity | 2.65 | - |
| Fineness modulus | 3.19 | - |
| Absorption % | 0.75 | - |

3.3.4 Hook-Ended Steel Fiber

The fiber used in this research was from BUNDREX KOSTEEL CO., LTD, which has been manufacturing steel fiber in Korea for the past 18 years as one of the global companies. Fiber Reinforced Concrete is made by incorporating steel fibers in different proportions of 1% and 0.5% by volume of cement. It is made of high tensile steel cold drawn wire with hooked ends

that has been specially designed for the use in concrete. Steel fibers conforming to ASTM A 820 type-I were used in the experiments. The type of Fiber is shown in Table 3-8 and Figure 3-5. The manufacturer in Korea provides this data. Newly developed steel fiber has extremely high tensile strength. It is an ideal concrete reinforcement that shifts the properties of concrete from brittleness to ductility, increasing toughness and resistance to cracking by reducing shrinkage[62].

Table 3-8: Properties of Steel Fiber type Hook Ended CH-65/35

| Properties | Value |
|-----------------------|--|
| Length of fiber | 35 mm |
| Diameter | 0.55 mm |
| Average aspect ratio | 65 |
| Appearance | Bright in clean wire |
| Deformation | Circular segment that is continuously deformed |
| Strength of tensile | 1500 MPa |
| Specific Gravity | 7.8 |
| Modulus of Elasticity | 210 GPa |

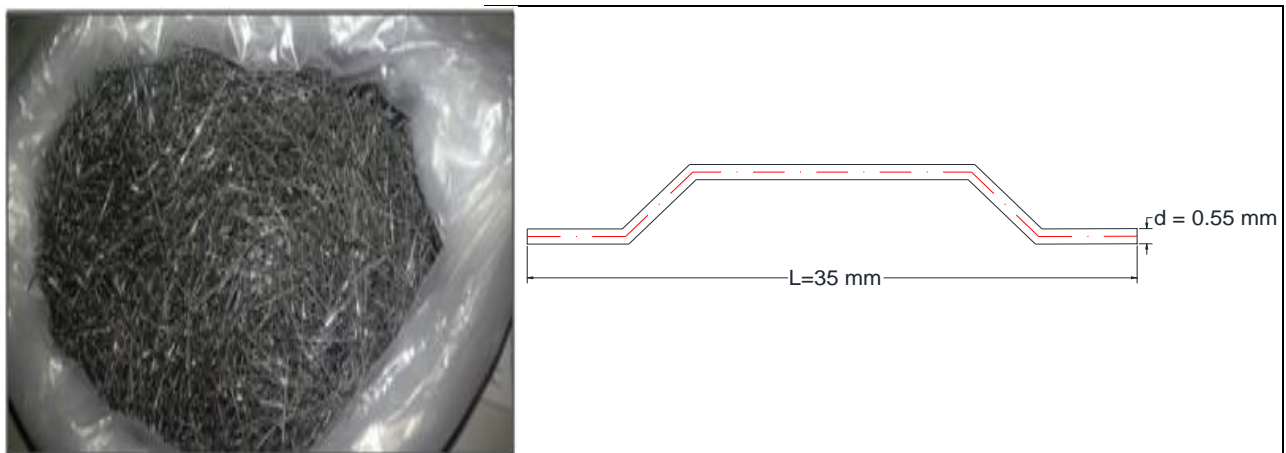
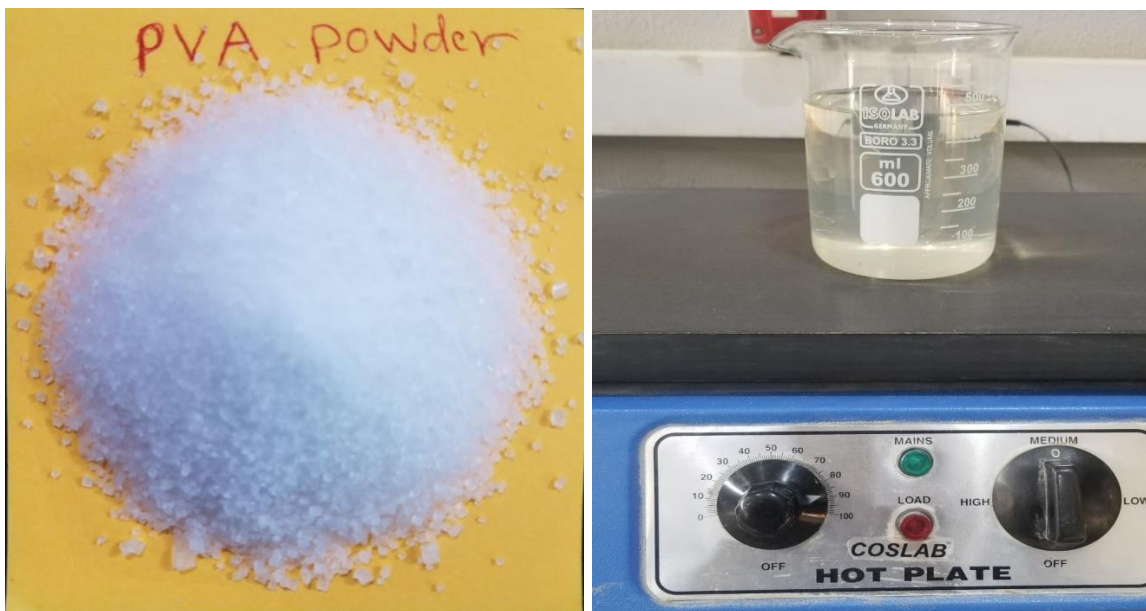


Figure 3-5: Hook Ended steel fiber CH-65/35

3.3.5 (PVA) Polyvinyl Alcohol

PVA's chemical formula (hereinafter occasionally referred to as PVOH, POVAL, or PVAL). PVA powder was used as a percentage of concrete weight. The Chang Chun petrochemical company provides equipment, 88% rated hydrolysis was used without further purification. It has a molecular weight of about 125,000 (mg/mol). In the form of a boiled powder in 300 ml of water at 90°C with agitation to completely dissolve the polymer. Significantly innocuous for capture and non-hazardous for comparatively environmentally friendly. PVA solution was translucent, tasteless, and odorless, as shown in Figure 3-6 after complete dissolution. The completely hydrolyzed grade types of PVA are soluble in hot water and have good film-forming characteristics. The film is insoluble in water at low temperatures and has good adhesive properties.



A) (PVA) Powder

B) (PVA) After completely dissolved.

Figure 3-6: Polyvinyl alcohol (PVA)

3.3.6 Reinforcement

All beams were reinforced with 12 mm and 6 mm of deformed steel reinforcement. The bottom main longitudinal reinforcement was 12 mm in diameter. At the same time, the top steel reinforcement was 6 mm in diameter. A diameter of 6 mm was chosen for shear reinforcement. Steel bar reinforcement tests were conducted in the Kerbala University Mechanical Engineering College Laboratory using a computerized testing machine, as shown in Figure 3-7. (ASTM A615M-05a) [54] was used to test the specimens. Steel reinforcement of 12 mm steel grade 40 and par 6 mm grade 75 technical requirements. Table 3-9 shows the mean data obtained from testing three specimens for each deformed bar.



Figure 3-7: Steel reinforcement testing machine

Table 3-9: Steel reinforcement properties

| Properties | Results | Tensile requirement ASTM 615M – 05a (Minimum) | Results |
|------------------------------|---------|---|----------|
| | | Ø12 | Grade 60 |
| Actual diameter (mm) | 11.80 | - | 5.78 |
| Nominal diameter (mm) | 12 | - | 6 |
| Yield stress, f_y (MPa) | 463.1 | $420 \geq$ | 675.7 |
| Elongation % | 18.2 | 9 % | 8.6 |
| Ultimate stress, f_u (MPa) | 591.1 | $550 \geq$ | 727.8 |

3.3.7 Carbon Fiber Reinforced Polymer (CFRP) Sheet

Reinforced concrete beam was strengthened with a (Nitowrap CW CWH 340 GPa) used had the dimensions (10 cm width, 160 cm length) shown in Figure 3-1; one unidirectional carbon fiber reinforced polymer (CFRP) sheet supplied by Fosroc as shown in Figure 3-8. The CFRP sheet was placed on the beam's bottom face using the Externally Bonded Reinforced technique (EBR). The carbon fiber-reinforced polymer (CFRP) sheet, a type of woven composite fabric used in this study. The advantages of the CFRP are; very high strength, outstanding fatigue resistance, non-corrosion, excellent alkali resistance, low weight, low thickness, available in any length, and economical to apply. The disadvantage is its relatively high material cost. The technical properties of the CFRP sheet given by the manufacturer Fosroc as shown in Table 3-10.

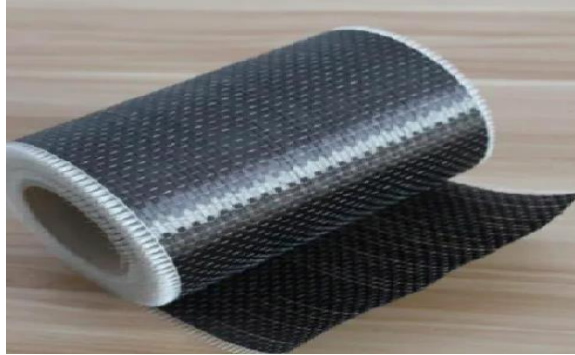


Figure 3-8: (Nitowrap CW CWH 340 GPa) CFRP sheet from Fosroc

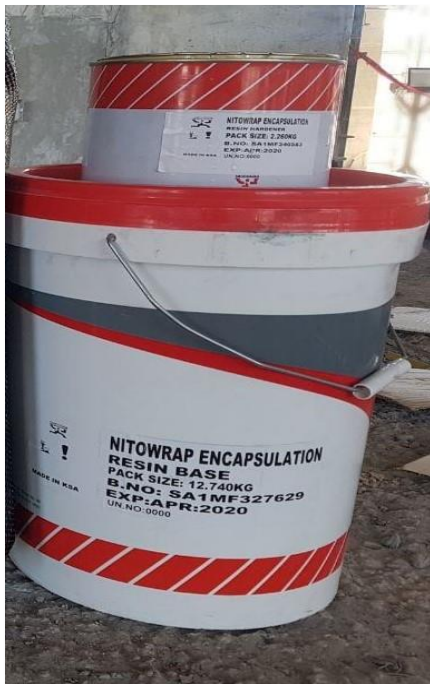
Table 3-10: Properties of (Nitowrap CW CWH 340 GPa) Carbon Fiber Sheets

| Properties | High strength carbon fibers |
|--|-----------------------------|
| Fiber Thickness | (0.167 mm) |
| Fiber Tensile Strength | >4600 (MPa) |
| Fiber orientation | 0° (unidirectional) |
| Fiber Density | (1.82 g/cm ³) |
| Fiber Modulus of Elasticity in Tension | >340 (GPa) |
| Fiber length/roll | 100 m |
| Fiber Elongation at Break | (1.4 %) |
| Fiber width | 500 mm |

3.3.8 Epoxy Resin

Carbon fiber reinforced plastic wrapping mechanism for epoxy reinforced concrete beams. Fosroc offers two types of epoxies; Nitowrap Primer and Nitowrap Encapsulation Resin. There are two ratios to mix the epoxy with the hardening material, the first ratio 58% of the total weight of epoxy (Nitowrap Primer) and the second ratio 48% of the total weight of epoxy (Encapsulation Resin). This epoxy was suitable for bonding due to its higher tensile strength than concrete, as illustrated in Table 3-11 and Figure 3-9. Any defects or holes discovered after the priming process should be filled

with the appropriate Nitowrap Primer as soon as possible. Apply Nitowrap Encapsulation resin at minimum consumption. Use a wet film thickness gauge to ensure the minimum thickness is achieved. Apply Nitowrap CW(CFRP) immediately after applying Nitowrap Encapsulation Resin. Carefully place Nitowrap CW on the substrate, ensuring tight contact with the substrate without air pockets. Use a ribbed lamination roller to remove burrs and air pockets and draw sufficient Nitowrap laminating resin to the surface. The manufacturer (Fosroc) provides this data.



a) Nitowrap Encapsulation Resin



b) Nitowrap Primer

Figure 3-9: (a ,b)Hardening and epoxy

Table 3-11: Properties of Nitowrap Primer and Nitowrap Encapsulation Resin

| Appearance | Nitowrap Primer | Nitowrap Encapsulation Resin |
|---|-----------------|------------------------------|
| Open time (mins) | 70 Minutes | 60 Minutes |
| Application temperature | +(10 ~ 40) °C | +(18 ~ 40) °C |
| Density (g/cm ³) | 1.8 | 1.8 |
| Flexural Strength | > 135 MPa | > 120 MPa |
| Tensile strength | > 38 MPa | > 37 MPa |
| Modulus of Elasticity in Flexure | > 4,900 | > 4,900 |
| Mixing ratio (Hardening and Epoxy) % | 0.58 | 0.48 |

3.3.9 Super-plasticizer (SP)

This Study used a high-range water-reducing (HRWR) admixture in the normal concrete (N.C) and the rest of the project's mixtures. Sika Company supplied it under the name (Sika ViscoCreteR-F180G) [55]. Sika ViscoCreteR F180G is a third-generation concrete and mortar admixture; it can be used to make various concrete types and can be utilized in both hot and cold weather conditions. This data is provided by the manufacturer, Sika, as shown in Table 3-12 and Figure 3-10. The properties of the super-plasticizer were found to meet the (ASTM C494) [56] super-plasticizer criteria for types G and F.



Figure 3-10: Sika ViscoCrete® F180G.

Table 3-12: Properties of Sika ViscoCrete®-F180G Technical Data

| Properties of Sika ViscoCrete® F180G. | Value and Description |
|--|--|
| Recommended dosage | (0.5 to 0.1) % litter by weight of cement for normal concrete (1 to 1.8) % litter by weight of cement for self-compacting concrete |
| PH | 4.5 - 6 |
| Appearance | Transparent/Turbid |
| Basis | Modified polycarboxylates based polymer |
| Density (kg / l L) | 1.061 |

3.4 Concrete Mixes

The main reference mix (N.C) with a compression resistance (f_c') of (30 MPa) has been chosen to achieve this compression strength target. Mixes for normal concrete have been carried out in the Kerbala Structural Laboratory

to choose the final mix design. These mixes have been designed using the (ACI 211.1) [51] Committee’s guidelines as shown in Table 3-13 the nine design mixes.

Table 3-13: Mix Properties of Concrete used

| mix materials | Types of concrete mixes used | | | | | | | | |
|---------------------|------------------------------|--------------------------|--------------------------|-------------------|-----------------|-----------------------------------|-------------------------------|---------------------------------|---------------------------------|
| | Reference mix (Mix 1) | Steel fiber (VF) (Mix 2) | Steel fiber (VF) (Mix 3) | PVA 1.2 % (Mix 4) | PVA 2 % (Mix 5) | 0.5 % (VF) with 1.2 % PVA (Mix 6) | 1 % (VF) with 2 % PVA (Mix 7) | 0.5 % (VF) with 2 % PVA (Mix 8) | 1 % (VF) with 1.2 % PVA (Mix 9) |
| (S. P) Ratio % | 1 % | 1.2 % | 1.2 % | 1.5 % | 1.5 % | 1.5 % | 1.5 % | 1.5 % | 1.5 % |
| (Kg/m3) | 3.8 | 4.56 | 4.56 | 5.7 | 5.7 | 5.7 | 5.7 | 5.7 | 5.7 |
| Steel Fiber (Kg/m3) | 0 | 6.483 | 12.958 | 0 | 0 | 6.483 | 12.958 | 6.483 | 12.958 |
| PVA (Kg/m3) | 0 | 0 | 0 | 4.56 | 7.6 | 4.56 | 7.6 | 7.6 | 4.56 |
| W/C=42% (Kg/m3) | 420 | | | | | | | | |
| Cement 1 (Kg/m3) | 380 | | | | | | | | |
| Gravel 2.81 (Kg/m3) | 1070 | | | | | | | | |
| Sand 1.97 (Kg/m3) | 750 | | | | | | | | |

3.5 Procedure for Mixing, Preparing and Casting Beams

Seventeen concrete beams of the same shape and dimensions were cast by ten moulds made of plywood with a thickness of 20 mm and clear dimensions (150 * 250 * 2,150) mm; a rectangular mould is formed of a hardwood bed and four sides attached to the bed with screws to form the framework of a plywood planks mould, as shown in Figure 3-11. The inner sides of the plywood formwork were oiled before inserting the reinforcement cage to ensure easy demolding.

The casting process is carried out in two batches in the University of Kerbala - construction laboratory. The first group consisted of nine beams, according to the mix design carried out in the laboratory. Refer to paragraph (3.2), where a beam is cast for each concrete mixture. The first beam was made of normal concrete, and the rest of the beams consisted of concrete with additives (steel fibers and polyvinyl alcohol solution). for this group, a laboratory mixer with a capacity of 0.14 m³ was used where the model was cast in one batch from the mixer, where the capacity of the whole beam(B.RC) was 0.0807 m³, in this way the first group was cast, as shown in Figure 3-12. As for the second group, known as 2YB.RC, it consisted of eight models and each concrete beam was cast in the form of two batches; the first part, which is deep in the tensile area, surrounds the reinforcing steel of the concrete beam, which is known as 2Y with a capacity of 0.017 m³, and its height is 52 mm, where this part was cast with concrete with additives (steel fibers and polyvinyl alcohol solution) by a small laboratory mixer with a capacity of 0.06 m³. After that, the trapped air was released by using a vibrator. As for the second part, cast into the mixer with a capacity of 0.14 m³, which is located above the tension area to the upper surface of the concrete beam. it was cast with normal concrete, where the thickness of the layer was 198 mm (250 mm

- 2Y), as shown in Figures 3-13 and 3-14, so casting the eight beams for the second group. Handling aggregate, casting, and curing concrete specimens was performed with ordinary clean tap water. The following points can sum up the casting steps for each group:

1) All of the materials for the concrete mix were weighed and placed in clean bags. Then an electric concrete mixer was used to mix gravel, sand, and cement with or without steel

fibers for more than two minutes, or until the mixture is homogeneous, according to the design composition.

Important note: Polyvinyl alcohol should be handled with caution when added to the mixture, as it was added to an appropriate amount of water and added to the mixture so that the mixture remains unsaturated with water and after mixing until homogeneity. The remaining water was added gradually because the solution causes air bubbles that settle and are difficult to be removed due to the nature of the substance [23].

2) Adding the ordinary clean tap water (Water designed for the mixture) gradually and leaving it to work until the mixture was completely homogeneous.

3) The concrete mixture was slowly cast vertically into a plywood mould. A trowel was used to raise the concrete surface. A vibrator was used to assist the trapped air in leaving. The samples were then covered with nylon to prevent water evaporation.

4) All samples were lifted and removed from their moulds after 24 hours. Following the removal of the formwork, all girders were stocked together, covered in burlap and nylon, and sprayed with water daily for up to 28 days. After the water treatment time, which is explained in Paragraph 3.18, a fortification was applied.

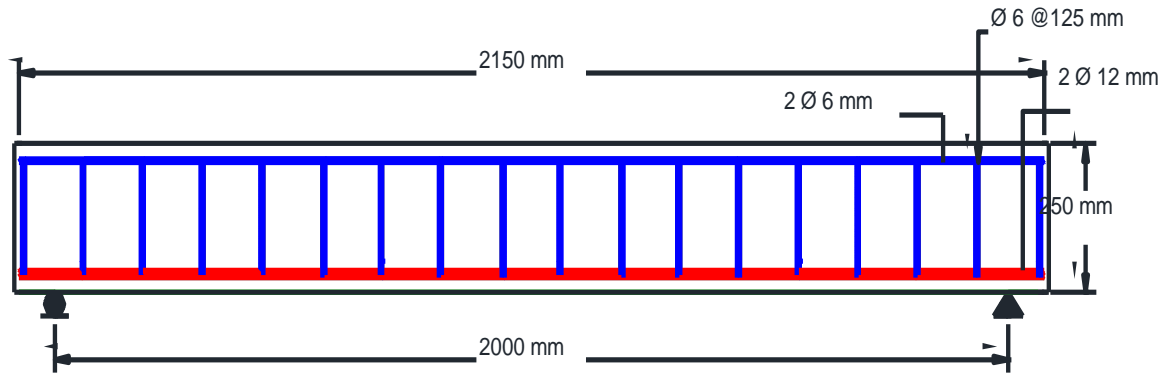
The concrete was formed in standard test moulds under conditions similar to girder sample casting. Samples of 9 cubes with dimensions of 10 *10 *10 cm and nine cylinders with diameters of 10 cm and lengths of 20 cm were tested and cast for each type of mixture. The samples were then covered with nylon to prevent water evaporation and raised for one day before being removed from the mould and soaked in water tanks for 7, 14, or 28 days depending on the test age. They were extracted from water and prepared for testing according to the test criteria.



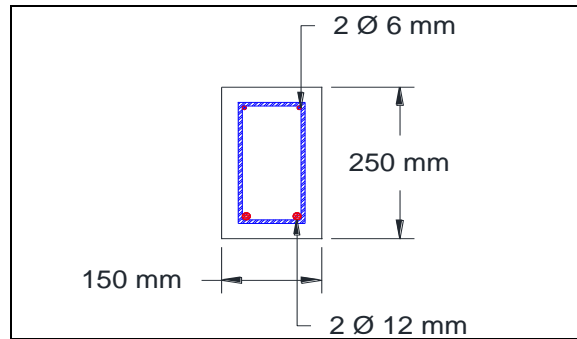
Figure 3-11: The plywood formwork with the reinforcement.



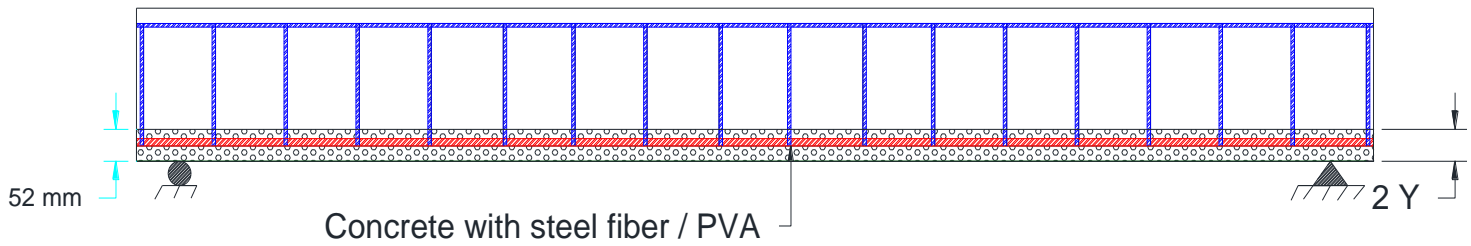
Figure 3-12: The first group where the model is casted in one batch from the mixer B.R.C.



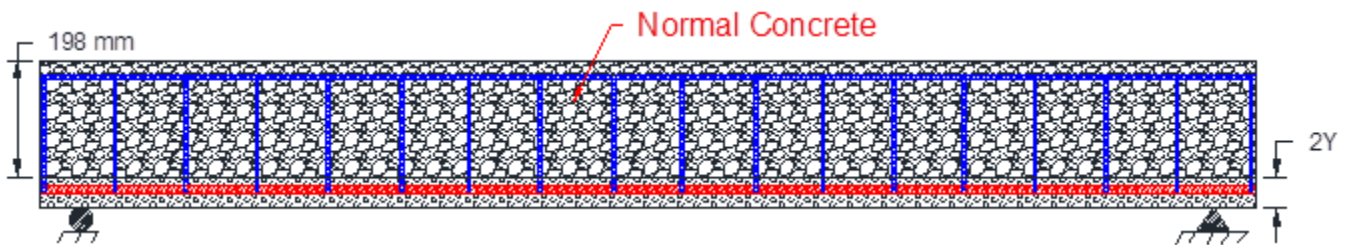
a) Preparing the model for casting with reinforcing steel in the mould



b) A cross section detailing the dimensions of the mold from the inside



c) Cast the bottom layer (52) mm of cured concrete (SFRC/PVA) and stack it with the vibrator



d) Pour the second layer (198) mm of regular concrete and stack it with the vibrator

Figure 3-13:(a,b,c,d) The second group 2YB.RC beam is casted in the form of two batches (2Y) and (250 mm - 2Y)

3.6 Bonding of Composite Materials to Beams

Unidirectional carbon fibers were added to concrete beams in the longitudinal direction to improve shear and flexural capacity and compare them to normal concrete (N.C), as shown in Figure 3-1. This procedure was completed in the Civil Engineering Laboratory over ten days before beginning to test the beams under flexural loads.

The concrete surface of the members that will be reinforced must be sound and clean. The bottom surfaces of the beams were cleaned with an electric hand grinder. After roughening the surface, dust was removed with air pressure and a brush. Figures 3-14 and 3-15 with cross-section area A-A show the surface preparation for CFRP installation after completion. All of the specimens were thoroughly washed and treated before applying the epoxy.

Carbon Fiber Reinforced Plastic (CFRP) panels are installed at the bottom of the concrete beam in the tension zone, which is the load concentration area on all cast beams. The following stages comprise the CFRP sheet installation process:

Stage 1: Clean the bottom surfaces of the beams with an electric hand grinder, removing any impediments between the concrete and the epoxy.

Stage 2: CFRP supplied by Fosroc (Nitowrap CW CWH 340 GPa) sheets were produced and cut into small sheets for each sample according to length requirements of 10*160 cm.

Stage 3: Composite material bonding to beams. A slow-speed electric drill was used to mix the epoxy. Two types of epoxies were used, as recommended by Fosroc (Nitowrap Primer and Nitowrap Encapsulation Resin):

a) A thin layer of (Nitowrap Primer) with a hardener/epoxy mixing ratio of 0.58 was applied to fill in any defects or holes discovered after the preparation process as quickly as possible.

b) A hardening ratio of 0.48 epoxy (Nitowrap Encapsulation Resin) was uniformly applied to the carbon fiber and the concrete substrate. Reinforced plastic was used to press fabric rolls against the concrete substrate. More epoxy was squeezed out and discarded. Before testing, samples were processed at room temperature for at least 24 hours.

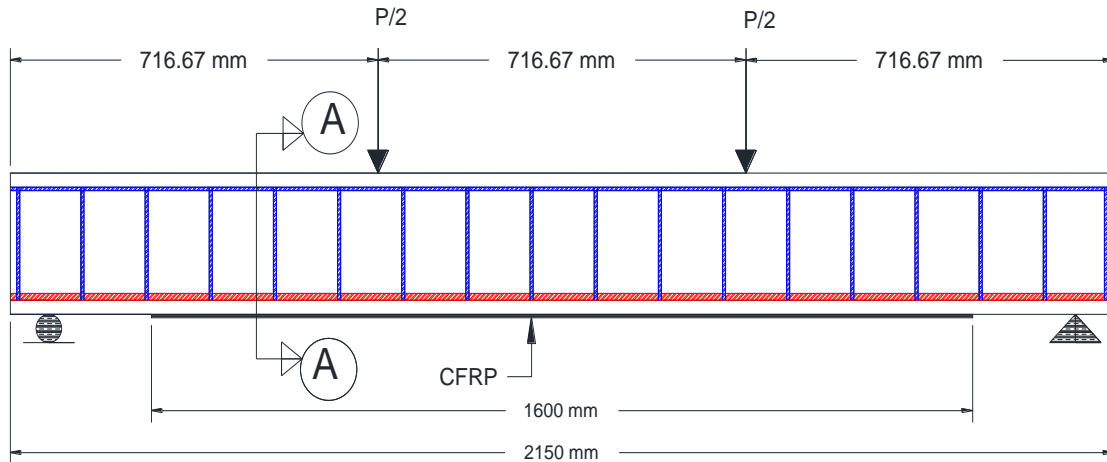


a) Skim the bottom surface and wash it in preparation for the epoxy primer



b) Apply a layer of epoxy primer c) Laying epoxy adhesive and applying CFRP

Figure 3-14:(a ,b ,c) CFRP sheet installation stages



a) Details and dimensions of the CFRP applied to the beam and loading details

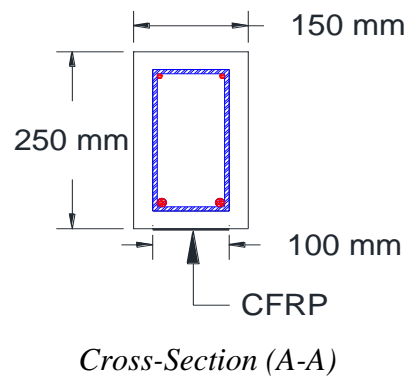


Figure 3-15: Schematic of CFRP sheet installation stages with cross-section (A-A)

3.7 Fresh Test and Hardened Testes

3.7.1 Slump Test and Density

Traditional slump test results have been used to determine the workability of nine concrete mixtures. The slump test was carried out using a truncated cone with a top diameter of 100 mm, a bottom diameter of 200 mm, and a height of 300 mm, as well as a tamping rod in conformity with ASTM 143M-12.[57] and the differences between them were acceptable. Wet and

dry densities were determined for nine different mixture samples, as indicated in Figure 3-16.



Figure 3-16: Slump test:

1) Normal concrete; 2) Concrete with steel fiber 1%.

3.7.2 Compressive and Splitting Tensile Strengths

The experiment was conducted on cubes aged 7, 14, and 28 days, with the findings were examined using digital pressure machine testing equipment with a capacity of 2000 kN. BS 1881: 1989, Part 116[58]. It was used to determine the compressive strength of concrete cubes (fcu). For each mixture, an average of three concrete cubes with dimensions of (100 x 100 x 100) mm was utilized to assess compressive strength. Three cubes of conventional concrete and SFRC-PVA concrete were tested for compressive strength. The

sample's compressive strength was calculated. A cylinder of (200 x100) mm was used for splitting tensile strength test in compliance with ASTM C496-11 [59] at 7,14, and 28 days. The cylinder was positioned horizontally between two plates of wood to evenly distribute the compressive machine's loads on the upper and bottom sides of the cylinder. A diametrical compressive force of 2000 kN was applied throughout the length of the specimen until the cylinder failed when a longitudinal crack split it in half. The splitting tensile resistance (ASTM C496) based on the average of three-cylinder samples. As indicated in Figure 3-17.



*Figure 3-17: Compressive and Splitting Tensile Strengths:
1) Compressive Strength; 2) Splitting Tensile Strength.*

3.8 Beams Configuration

All beams were reinforced similarly by adding one layer of carbon-fibre-reinforced plastic CFRP to the bottom of the concrete beam.

The cross-sectional area of seventeen beams was identical in length and reinforcement details but differs in two significant ways: the method of casting the concrete beam and the type of concrete used to cast each beam. Except for the first beam, which serves as a control beam, the beams were divided into eight sections based on the type of concrete used. The eight beams' details are mentioned in Table 3-14, along with their names based on the method of casting and the type of concrete used.

Table 3-14: Description of the Specimens

| The first group Method of casting the beam in one batch of concrete | Sample Description | The second group Method of casting the girder in two batches of concrete | Sample Description |
|--|-------------------------------|---|-------------------------------|
| Control Beam | C.B | | |
| Beam with steel fiber 0.5% | BS 0.5 | Beam with steel fiber 0.5% | 2YBS 0.5 |
| Beam with steel fiber 1% | BS 1.0 | Beam with steel fiber 1% | 2YBS 1.0 |
| Beam with PVA solution 1.2% | BPV 1.2 | Beam with PVA solution 1.2% | 2YBPV 1.2 |
| Beam with PVA solution 2% | BPV 2.0 | Beam with PVA solution 2% | 2YBPV 2.0 |
| Beam with steel fiber 0.5% & PVA solution 1.2% | BSPV 0.5.1.2 | Beam with steel fiber 0.5% & PVA solution 1.2% | 2YBSPV 0.5.1.2 |
| Beam with steel fiber 1% & PVA solution 2% | BSPV 1.0.2.0 | Beam with steel fiber 1% & PVA solution 2% | 2YBSPV 1.0.2.0 |
| Beam with steel fiber 0.5%& PVA solution 2% | BSPV 0.5.2.0 | Beam with steel fiber 0.5%& PVA solution 2% | 2YBSPV 0.5.2.0 |
| Beam with steel fiber 1%& PVA solution 1.2% | BSPV 1.0.1.2 | Beam with steel fiber 1%& PVA solution 1.2% | 2YBSPV 1.0.1.2 |

3.9 Test Procedures and Experimental Setup

All beams were tested using a flexural machine at University of Kerbala - Construction Laboratory. Some changes have been made to the testing machine to make it more useful for testing beams, such as using a steel frame as a support. Each beam has a partially simply supported end. As illustrated in Figure 3-18, two-points loads were applied at the mid-span of the beam. After 28 days of casting, the beam specimens were removed from the water after the samples had finished curing. Then it was cleaned and white-painted to clarify cracks and distinguish failure modes. The recorded data was used to monitor the loading and the mid-span deflection. The program Lab VIEW 2018 was used to connect the LVDTs of 10 cm settlement capacity to monitor the mid-span deflection and load cell that was linked to a computer. A hydraulic jack applies the load, and a load cell measures it. Two marks were placed 75 mm from the ends of the beam to determine the location of the simple support, and a third mark was placed below the center of the beam. Figure 3-19 shows that a machine with a maximum capacity of 2000 kN was available in the Civil Engineering Department Engineering College at the University of Kerbala's concrete laboratory. The load was gradually applied until the beam failed. For simple support, the load increment was around 1 kN. For accuracy and comparing purposes, the load was recorded using a load cell with a capacity of 2000 kN linked to a computer. The load was applied gradually at two points spaced 716.7 mm apart in the middle of the beam until the failure of the beam. The number of cracks and the load corresponding to the appearance of each crack in the beam were observed.

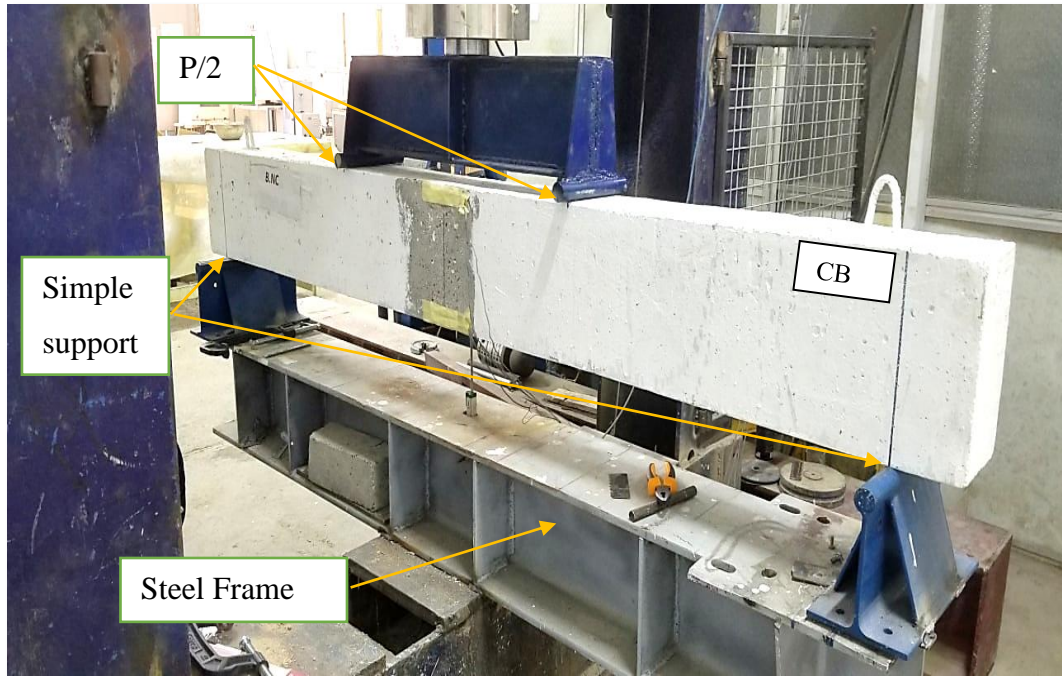


Figure 3-18: Flexural testing machine with support and loading details, (at Kerbala Construction Laboratory)

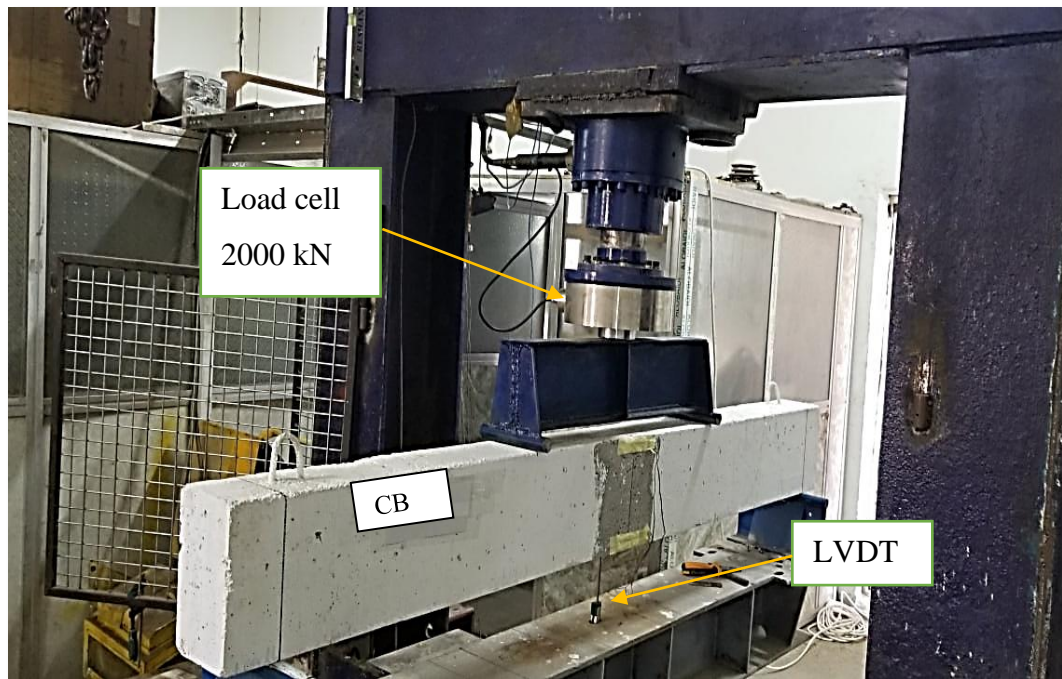


Figure 3-19: Flexural testing machine with the details of the gauges, (at Kerbala Construction Laboratory).

Chapter Four: Results

Chapter Four: Results and Discussion

4.1 Introduction

The Seventeen tested beams were designed to fail under flexure using the minimum reinforcement ratio (Appendix A) recommended by ACI-318M-11.[51]. Therefore, 2 Φ 12 mm steel bars were considered the beams' main flexural reinforcement. Also, Φ 6 mm stirrups spaced at 125 mm c/c were used for shear reinforcement. The test results described in chapter three are presented and discussed in this chapter. These results are divided into the following main parts:

Part one: displays the test results of fresh and hardened properties of concrete composites PVA solution with steel fiber (PVA- SFRC concrete). Fresh and hardened concrete properties include slump test, fresh and hardened concrete densities, compressive strength, and tensile strength.

Part two: Presents the results of the mechanical properties of the concrete composite containing steel fibers (SFRC) with and without PVA material, which are flexural strength versus load-deflection relationship at the age of 28 days.

4.2 Fresh Concrete Properties

4.2.1 Workability (Slump Values), Super-plasticizer (SP), and Density

The results of Density and slump test values used to measure the workability of nine concrete mixes are shown in Table 4-1. The Super Plasticizer (SP) was utilized in this investigation to keep the workability as close as possible to a similar slump range.

Table 4-1: Concrete properties of all mixes

| Mix type | Slump value (mm) | %Difference compared to (NC) | % (SP) | Wet Density (kg/m ³) | Dry Density (kg/m ³) |
|--------------|------------------|------------------------------|--------|----------------------------------|----------------------------------|
| N.C | 70 | 0.00 | 1.0 | 2468 | 2423 |
| VF 0.5 | 100 | + 42.86 | 1.2 | 2516 | 2444 |
| VF 1 | 80 | + 14.29 | 1.2 | 2529 | 2453 |
| PV 1.2 | 100 | + 42.86 | 1.5 | 2503 | 2432 |
| PV 2 | 100 | + 42.86 | 1.5 | 2480 | 2381 |
| VFPV 0.5.1.2 | 100 | + 42.86 | 1.5 | 2554 | 2450 |
| VFPV 1.0.2.0 | 95 | + 35.71 | 1.5 | 2554 | 2448 |
| VFPV 0.5.2.0 | 90 | + 28.57 | 1.5 | 2508 | 2422 |
| VFPV 1.0.1.2 | 90 | + 28.57 | 1.5 | 2560 | 2467 |

The experimental result showed that slump values of fresh concrete containing SFRC-PVA were in the limit range between 80 mm - 100 mm (Table 4-1) compared to the 70 mm slump for normal concrete (N.C), and the differences between them were acceptable. According to the results, the workability decreased as the volumetric ratio of steel fiber and PVA material increased. Steel fibers changed the properties of hardened concrete significantly. Thus, the addition of fibers to new concrete resulted in a loss of workability. Fibers with hooked ends cause blocking of particles during the slump tests. The magnitude of this effect depends on fiber content in the

mixture [60]. A higher percentage of PVA leads to lower workability of the slurry due to the increase of slurry viscosity [61]. Super-plasticizer (SP) helps to disperse fibers evenly during mixing and reduces the internal friction in fresh concrete, increasing the flow ability and compaction of that concrete [60]. The workability can be controlled by changing the percentage of plasticizer range (1-1.5%). The percentage of super-plasticizer that -specified the slump value was in the limit of specification. The densities of Concrete mixes (SFRC-PVA) might be increased or decreased due to the nature of the material. The following are the reasons for increase the density of the concrete:

1-Adding steel fibers with high specific gravity to ordinary concrete.

2-Using 1.2% of Polyvinyl alcohol (PVA) increases viscosity and intermolecular attraction and reduces porosity.

The results indicate that the Density decreased when 2% of PVA was added to the mix. This is due to the nature of the alcoholic substance in forming bubbles, which are challenging to get rid of through compaction. The remaining bubbles create voids inside the concrete mix that lead to a reduction in Density.

4.3 Hardened Concrete Properties

Understanding the behavior of SFRC-PVA concrete requires knowledge of its mechanical characteristics. As a result, hardened characteristics tests such as compressive strength and splitting tensile have been carried out.

4.3.1 Compressive Strength of SFRC-PVA Concrete

The compressive strength increased when polyvinyl alcohol and steel fibers were added to normal concrete ($w/c = 0.45$) as indicated in Table 4-2.

Adding 1.2% polyvinyl alcohol with 1% steel fiber achieved concrete with highest compressive strength; the percentage of increase was 65.31% compared to normal concrete (N.C) mixes when checking the compressive strength at 28 days. Nevertheless, the lowest increase in compressive strength 3.9%, at 28 days, was obtained when 2% of polyvinyl alcohol was added. As an average, three cubes were taken to obtain compressive strength at 7, 14, and 28 days. The effect of PVA on the compressive strength is due to the chemical reactions between PVA and cement, as a new chemical may also be developed that can enhance the bonding between the cement particles [60]. The chemical reaction between PVA and cement particles results in various new products to fill voids in the mortar composite and increase the bonding between cement particles [20]. However, a mix of 2% of PVA shows low resistance due to increased air inside the concrete mix. When cement and aggregates are combined with an aqueous polymer solution, air voids emerged, which are difficult to be removed since the polymer tends to harden them. Small air gaps generated during the mechanical combination period can be connected to form larger air voids, resulting in surface climb and ruptures [23]. With the addition of hooked end steel fiber, the compressive strength of the concrete improves compared to plain concrete. It was found in this study that increasing steel fiber from 0.5% to 1% increases compressive strength by 19.15%.

Table 4-2: The average results of compressive strength.

| Mix type | % Of VF | % (PVA) (p/c) | Av. Compressive strength (MPa) | | |
|--------------|---------|---------------|--------------------------------|---------|---------|
| | | | 7 days | 14 days | 28 days |
| N.C | 0.0 | 0.0 | 18.23 | 25.20 | 34.36 |
| VF 0.5 | 0.5 | 0.0 | 25.11 | 32.46 | 42.29 |
| VF 1 | 1.0 | 0.0 | 34.40 | 41.76 | 48.87 |
| PV 1.2 | 0.0 | 1.2 | 20.38 | 30.87 | 40.50 |
| PV 2 | 0.0 | 2.0 | 18.36 | 25.97 | 35.70 |
| VFPV 0.5.1.2 | 0.5 | 1.2 | 37.03 | 48.70 | 53.60 |
| VFPV 1.0.2.0 | 1.0 | 2.0 | 40.37 | 49.83 | 55.30 |
| VFPV 0.5.2.0 | 0.5 | 2.0 | 35.20 | 46.03 | 50.20 |
| VFPV 1.0.1.2 | 1.0 | 1.2 | 42.34 | 52.40 | 56.80 |

4.3.2 Splitting Tensile Strength

The results of tensile strength for the nine different mixes are listed in Table 4.3. The outcomes indicated that the tensile resistance values increased as the steel fiber ratio increased. The failure mode of the reference mix (N.C) was a brittle failure, where the cylinder split into two sections. On the other hand, other concrete combinations with additives did not have this failure mode. The failure mode of steel fiber and PVA concrete mixtures was due to the vertical cracks along the diameters of the cylinders[49] [50], as shown in Figure 4-1. The tensile strength value of the steel fiber concrete sample increased with PVA polyvinyl alcohol solution compared to the normal concrete (N.C) mixes. The ideal ratio was 1.2% PVA with 1% steel fiber, which shows a 73% increase in tensile resistance. According to the findings, the increase in compressive strength values was similar to the increase in splitting tensile resistance.

Table 4-3: Results of the average tensile strength

| Mix type | Tensile strength (ft) MPa | | |
|--------------|---------------------------|---------|---------|
| | 7 days | 14 days | 28 days |
| N.C | 2.76 | 3.18 | 3.51 |
| VF 0.5 | 3.55 | 4.31 | 4.84 |
| VF 1 | 4.39 | 4.96 | 5.28 |
| PV 1.2 | 3.06 | 3.60 | 4.21 |
| PV 2 | 2.86 | 3.37 | 3.83 |
| VFPV 0.5.1.2 | 4.52 | 5.10 | 5.55 |
| VFPV 1.0.2.0 | 4.59 | 5.37 | 5.82 |
| VFPV 0.5.2.0 | 4.46 | 4.95 | 5.70 |
| VFPV 1.0.1.2 | 4.88 | 5.67 | 6.10 |



Figure 4-1: Mode of Failure of Various Mixtures in Splitting Test,

a): NC, b): PVA-0.5% steel fibers, c): PVA-1% steel fibers

4.4 General Behavior of Tested Beams

4.4.1 Beams Cast into one batch (Group 1)

This group (group 1) consists of nine reinforced concrete beams, one of these beams was cast as one unit (one batch of concrete) without SFRC-PVA to be used as a reference for comparison purposes. The other eight beams were concrete with SFRC-PVA but with different percentages of SFRC-PVA added to ordinary concrete, as elaborated in chapter 3. The results of all specimens that include the first crack, ultimate load, max deflection, and failure modes are illustrated in Table 4-4.

Table 4-4: Results of the tested beams-group 1

| Beam symbol* | First flexural crack load (Pcr) (kN) | Ultimate load (Pu) (kN) | $\Delta\% *$ | Max. deflection (mm) | Type failure |
|--------------|--------------------------------------|-------------------------|--------------|----------------------|----------------------|
| C.B | 17 | 85.25 | 0.000 | 20.15 | Delamination failure |
| BS 0.5 | 21 | 100.92 | 18.381 | 22.76 | Delamination failure |
| BS 1.0 | 23 | 110.22 | 29.290 | 24.09 | Debonding failure |
| BPV 1.2 | 20 | 97.22 | 14.041 | 21.90 | Debonding failure |
| BPV 2.0 | 19 | 93.38 | 9.536 | 21.50 | Delamination failure |
| BSPV 0.5.1.2 | 25 | 119.25 | 39.882 | 24.70 | Debonding failure |
| BSPV 1.0.2.0 | 26 | 124.40 | 45.923 | 26.07 | Debonding failure |
| BSPV 0.5.2.0 | 23 | 114.80 | 34.662 | 24.36 | Debonding failure |
| BSPV 1.0.1.2 | 29 | 131.50 | 54.252 | 27.03 | FRP rupture |

$$\Delta\% * = \frac{Pu(i) - Pu(R)}{Pu(R)} * 100\%$$

4.4.2 Beams Cast into Two Batches Group 2 (2YB.RC)

This group (group 2) also comprises nine reinforced concrete beams. The first specimen was cast to have one unit without SFRC-PVA as a

reference beam. Whereas the other eight beams were referred to as 2YB.RC (Figure 3-13). Each concrete beam was cast in two parts. The first part was cast from the bottom of the beam to a height of 52 mm (2Y), as shown in Figure 3-13. This part was cast using concrete with steel fibers and polyvinyl alcohol solution. The second part, located above the 52 mm (2Y) till the upper surface of the concrete beam, was cast with ordinary concrete. Table 4-5 summarizes the results for this group, including first cracks, ultimate load, maximum deflection, and failure modes.

Table 4-5: Results of the tested beams group 2

| Beam symbol* | First flexural crack load (P_{cr}) (kN) | Ultimate load (P_u) (kN) | Δ% * | Max. deflection (mm) | Type failure |
|---------------------|--|---|-------------|-----------------------------|----------------------|
| C.B | 17 | 85.25 | 0.000 | 20.15 | Delamination failure |
| 2YBS 0.5 | 19 | 96.60 | 13.313 | 22.44 | Delamination failure |
| 2YBS 1.0 | 21 | 103.70 | 21.642 | 22.88 | Debonding failure |
| 2YBPV 1.2 | 18 | 93.30 | 9.442 | 21.42 | Delamination failure |
| 2YBPV 2.0 | 18 | 88.70 | 4.046 | 21.28 | Delamination failure |
| 2YBSPV 0.5.1.2 | 23 | 115.88 | 35.929 | 24.02 | Debonding failure |
| 2YBSPV 1.0.2.0 | 26 | 117.34 | 37.642 | 25.07 | Debonding failure |
| 2YBSPV 0.5.2.0 | 22 | 110.90 | 30.087 | 23.46 | Delamination failure |
| 2YBSPV 1.0.1.2 | 27 | 125.60 | 47.331 | 25.76 | Debonding failure |

The following part will present a study on flexural behavior in terms of first crack load, ultimate load, load-deflection curves, crack pattern, and failure mode.

4.5 Effect of Test Parameters

These parameters' effects are briefly described in the following sections (4.5.1 to 4.5.2.2).

4.5.1 Studying the effect of parameters for Group One

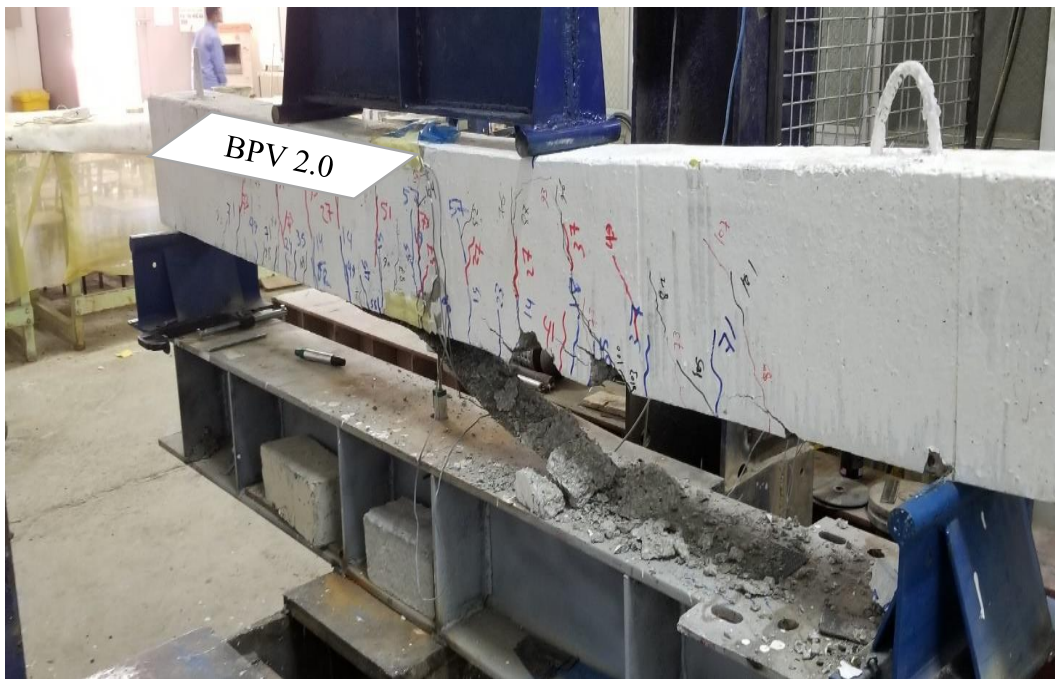
This group contained a total of nine beams and each beam was cast with one mixer. The comparison was made between the control beam and other beams that strengthened with CFRP in terms of the maximum deviation at failure. The failure occurred after the carbon fibers disengaged from the beams.

4.5.1.1 Effect of Polyvinyl Alcohol Solution on Beams Control

The mid-span deflection was measured for both the control specimen and the beam containing the polyvinyl alcohol solution. The experimental results revealed that the deflection of the PVA beams BPV 1.2 and BPV 2.0 at the ultimate load was higher than those of the control beam (C.B) by 8.68% and 6.69%, respectively. It was also observed that the ultimate load of the PVA beams were 14.04% and 9.54% greater than the control beam (C.B), respectively. The failure of the beam BPV 2.0 by delamination (removing the cover with removing CFRP sheet) Figure 4-2, showed a less loading than the BPV 1.2 beam, while the problem of debonding appeared in the BPV 1.2 beam and it occurred when the load reached 97.22 kN. Figure 4-3 depicts the curve of load deflection in mid-span for the control beam (C.B) and the PVA concrete beams.



a) *The failure of the beam BPV 1.2 by debonding problem*



b) *The failure of the beam BPV 2.0 by delamination problem*

Figure 4-2: Failure modes (PVA)concrete a): Beam PVA 1.2%, b): Beam PVA 2%

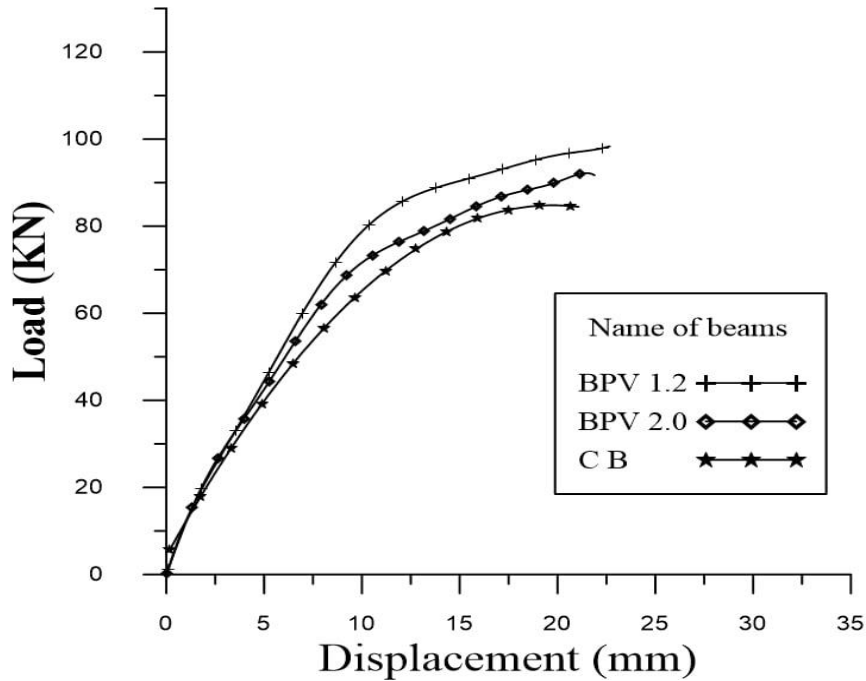
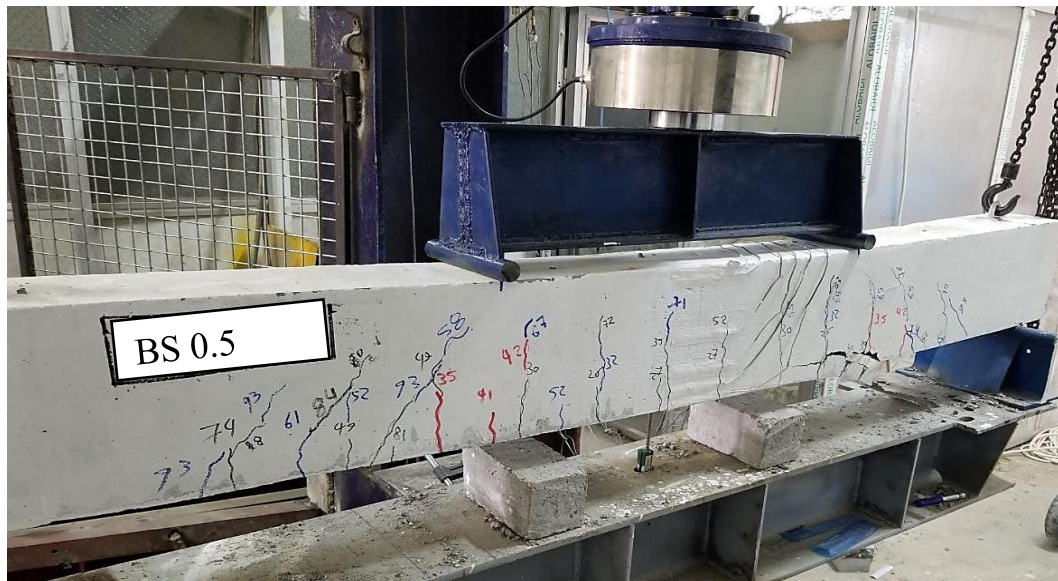


Figure 4-3: PVA load versus deflection -Group1

4.5.1.2 Effect of Hook Steel Fiber on Control Beam

The experimental results demonstrated that substituting SFRC for N.C could enhance the overall behavior of the beams. Two percentages of steel fiber volume were considered with ratios of 0.5% and 1% of the cement volume. Expanding the volumetric percentage of steel fiber from 0.5% to 1% in BS 0.5 and BS 1.0 beams enhanced the ultimate load by about 18.38% and 29.29%, respectively, compared to the control beam (C.B) by using N.C. At the ultimate load (BS 0.5 and BS 1.0), the deflection was greater than those of control beams (C.B) by N.C, using 12.95% and 19.55%, respectively. Figure 4-5 shows the effect of SFRC on the load-deflection curves of the control beam (C.B). When the steel fiber percentage for ordinary concrete was improved from 0.5% to 1%, the ultimate load of the SFRC beam increased by 10.91%, while the deflection improved by approximately 6.6%. It was noticed from Figure 4.4 that using SFRC increased the stiffness and the ductility of

the control beam (C.B). As a result, there was a noticeable improvement in the general behavior of the control beam (C.B), especially when the steel fibers ratio was increased from 0.5% to 1%. The failure of the beam BS 1.0 by debonding problem and BS 0.5 by cover delamination problem and showed a higher loading than the control beam (C.B) Figure 4-4.



a) Failure of the beam BS 0.5 by delamination problem



b) Failure of the beam BS 1.0 by debonding problem

Figure 4-4: Failure modes (SFRC)concrete a): Beam BS 0.5 b): Beam BS 1.0

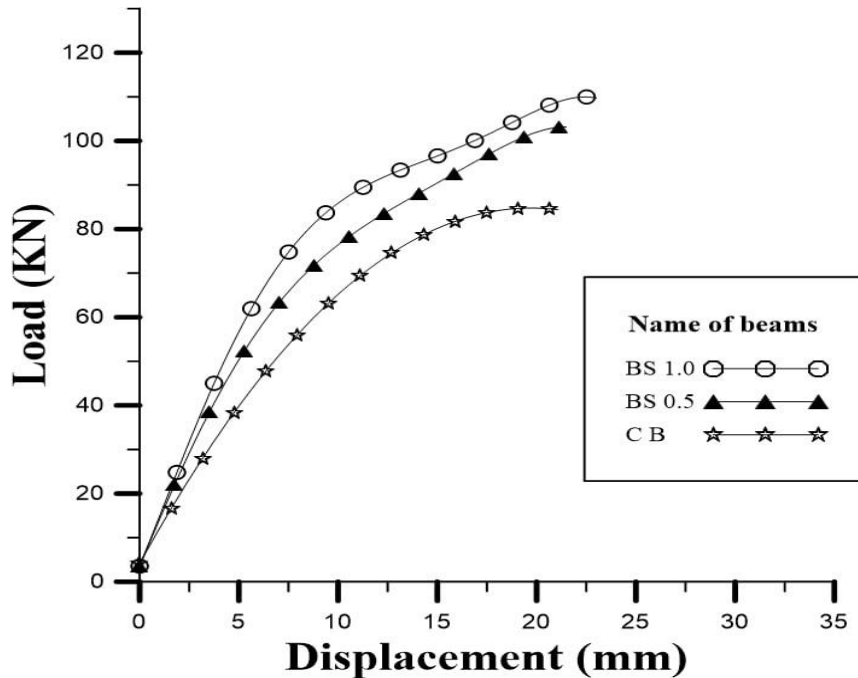


Figure 4-5: SFRC load versus deflection -Group 1

4.5.1.3 Effect of PVA and Steel Fiber (SFRC-PVA) on Control Beam

To improve the concrete's compressive strength and tensile strength, a mixture of SFRC and PVA was utilized in place of normal concrete N.C in the beam. Ratios of 0.5 % and 1% were used as the volume of steel fibers in SFRC. In addition, two ratios of 1.2% and 2% from polyvinyl alcohol solution PVA were added. The ratios were considered from the volume of cement only to evaluate the effect of the added percentages. Four mixtures of these ratios were used, and the best of these mixtures was determined to improve the properties of concrete and reduce the decoupling between concrete and CFRP. These mixtures were classified in two cases according to the mixing ratios of each additive as follows:

Case 1: BSPV 0.5.1.2 and BSPV 0.5.2.0 beams compared to the control beam.

The mid-range deflection was measured for the control and the beam containing (SFRC-PVA). It was found from the experimental results that the

deflections of beams BSPV 0.5.1.2 and BSPV 0.5.2.0 at the final load were higher than the deflection of the control beam (C.B) by 22.58% and 20.89%, respectively. The peak loads for those beams were 39.88% and 34.66%, respectively, greater than the control beam (C.B). Adding polyvinyl alcohol with steel fibers (SFRC-PVA) to the cement matrix improved the bonding and helped spread the load over a larger area in the tensile zone because of the bridging phenomenon that occurs in steel fiber concrete. Figure 4.6 demonstrates the curve of load deflection for the control beam (C.B), beam BSPV 0.5.1.2, and beam BSPV 0.5.2.0 and the failure of this beam's cues by debonding problem Figure 4.7.

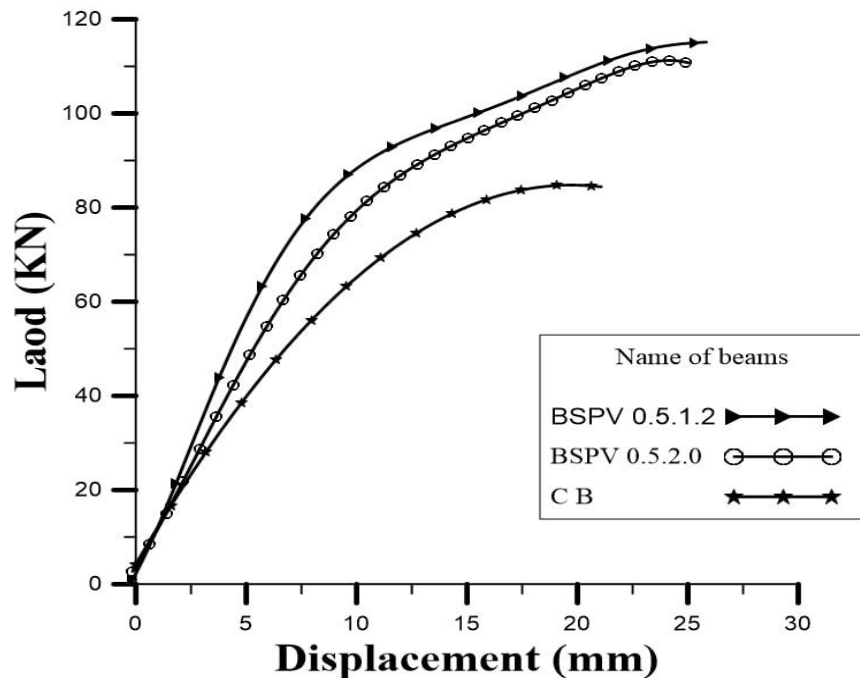


Figure 4-6: Case 1: SFRC-PVA load versus deflection

Case 2: BSPV1.0.2.0 and BSPV 1.0.1.2 beams compared to the control beam.

The mid-range deflection was measured for the control beams and the beam with SFRC-PVA. From the experimental results, the deflection of beams BSPV 1.0.2.0 and BSPV 1.0.1.2 at the failure was higher than the deflection of the control beam (C.B) by 29.38% and 34.14%, respectively. Also, the ultimate load for specimen BSPV 1.0.2.0 was 45.92%, and 54.25% for the BSPV 1.0.1.2. The load-deflection curves of the control beam (C.B) and BSPV 1.0.2.0, and BSPV 1.0.1.2 are shown in Figure 4-8. Failure of the beams in both cases (case 1 and case 2) by debonding problem showed a higher loading than the control beam (C.B). The failure of the beam BSPV 1.0.2.0 by debonding problem, Figure 4-9, showed a less loading than the BSPV 1.0.1.2 beam, while the problem of FRP rupture appeared in the BSPV 1.0.1.2 beam.

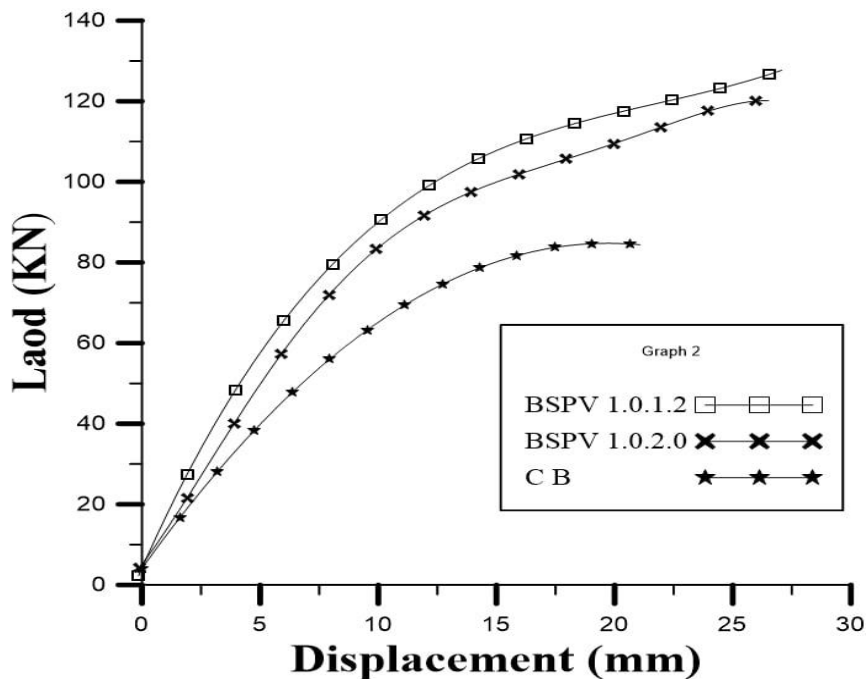


Figure 4-8: SFRC-PVA load versus deflection - Case 2

(BSPV 1.0.1.2) and (BPV1.2). It has been proven that adding 1.2% PVA with 1% SFRC by weight/volume of cement to the mixture improves the bonding strength between carbon beam and carbon fiber compared to all other beams.

4.5.2 Study the effect of parameters on Group Two

Each beam in this group was cast with two mixers. This set consisted of eight beams, including the control beam cast in one batch. The comparison was made between the control beam (C.B), the beams from group one, and the present beams (with two batches). The comparison included the amount of maximum deflection, the maximum loading moment of failure, and the load response.

All the beams had the same CFRP strengthening. It was observed that all the strengthened beams failed after the carbon fibers separated from the beams.

4.5.2.1 Effect of PVA on the Beams that were Cast in Two Batches

The deflection results showed that the beams cast as one layer with PVA additive in the bottom layer (2Y) region had higher deflection than the control beam (C.B). The deflection for the beams 2YBPV 1.2 and 2YBPV 2.0 at the final load were 6.30% and 5.61%, respectively, higher than the control beam. In comparison with the control beam, the increase in the final load for specimen 2YBPV 1.2 was 9.44%, and 4.05% for beam 2YBPV 2.0. Beam 2YBPV 1.2 had a higher load capacity than beam 2YBPV 2.0 (Figure 4-10), similar to the beams in the first group that were cast as one unit.

When comparing the PVA beams of the second group (2YBPV) with (BPV) beams of the first group, the deviations of BPV 1.2 and BPV 2.0 beams were higher than that of the beams of the second group 2YBPV 1.2 and 2YBPV 2.0 by 2.38% and 1.08%, respectively. The increase in the maximum

load for the first group was 4.6% and 5.49%, respectively, compared to the second group, as shown in Figures 4-8 and 4-9.

It was noted that the (2YBPV) beams in the initial loading stages had a stiffness factor greater than that for the (BPV) beams. This was due to casting the second batch in two layers. A vibrator compacted each layer to remove the air bubbles that formed from mixing the fresh concrete and from the action of PVA. Since PVA is an alcoholic substance, it tends to form air bubbles when mixed with water. Casting the beams 2YBPV in two layers may cause a construction joint that allows for some horizontal movement. At a higher load level, the deflection curve began to descend below the deflection curve of the beams in the first group, as seen in Figures 4-12 and 4-13. The reason for this descent is the transfer of loads from high-strength concrete to lower-strength concrete, as well as the presence of the connecting area between the two layers. The failure of the beams (2YBPV 2.0 and 2YBPV 1.2) by delamination (removing the cover with removing CFRP sheet) Figure 4-11.

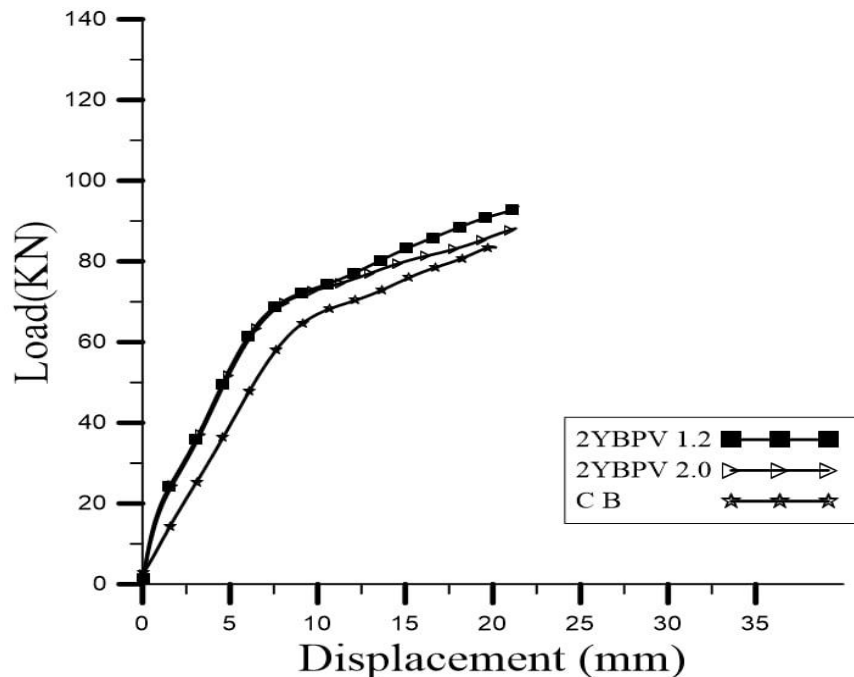


Figure 4-10: PVA load versus deflection -Group 2



a) *The failure of the beam by cover delamination*



b) *The failure of the beam by cover delamination*

Figure 4-11: Failure modes (2Y PVA) concrete a): Beam 2YBPV 2.0

b): Beam 2YBPV 1.2

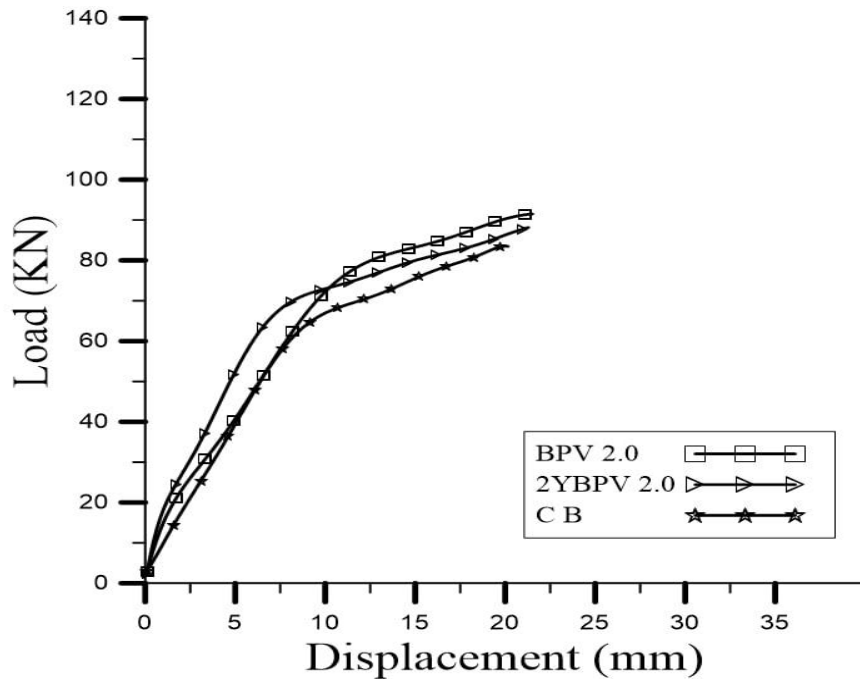


Figure 4-12: PVA 2% load versus deflection - compared Group 2 with Group 1

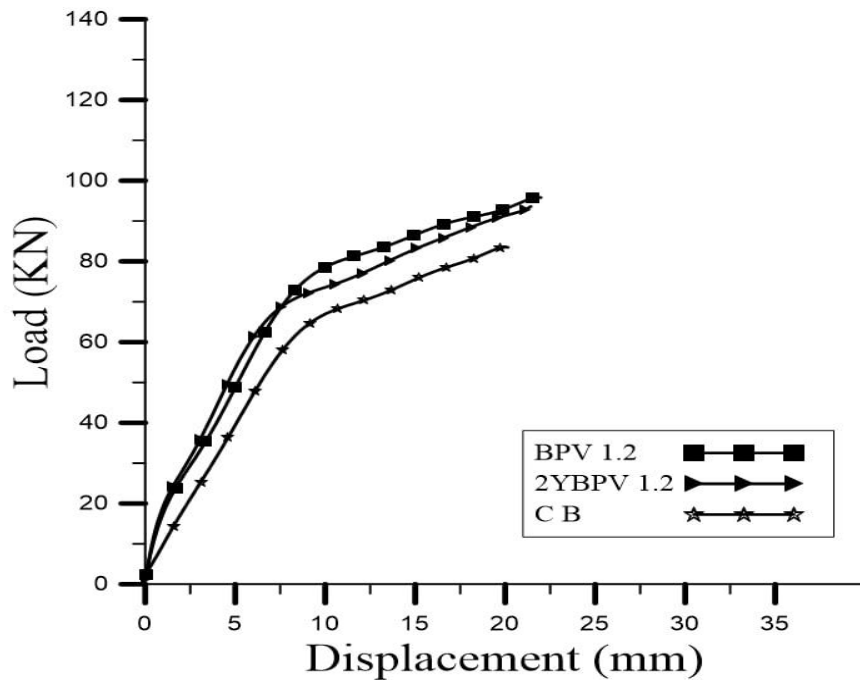


Figure 4-13: PVA 1.2% load versus deflection - compared Group 2 with Group 1

4.5.2.1 Effect of Bottom Layer Steel Fiber on the Beams Cast in Two Batches

The SFRC mixture was used in the area around the steel rebar (2Y), which increased the deflection at the mid-range of the beam (2YBS 0.5 and 2YBS 1.0) by 11.36% and 13.55%, and the maximum load was increased by about 13.31% and 21.64%, respectively compared to the control beam. Also, increasing the percentage of steel fibers in the area (2Y) from 0.5% to 1% led to an increase in the final load by 8.33%, compared to the ordinary concrete as shown in Figure 4-14. The failure of the beam 2YBS 1.0 by debonding problem and 2YBS 0.5 by cover delamination problem and showed a higher loading than the control beam (C.B) Figure 4-15.

When comparing the beams BS with 2YBS, it was found that the increase in the load in the beams (BS 0.5 and BS 1.0) compared with (2YBS 0.5 and 2YBS 1.0) was 4.47% and 6.29%, and the maximum deviation increased by 1.43% and 5.29% respectively, as shown in Figures 4-16 and 4-17.

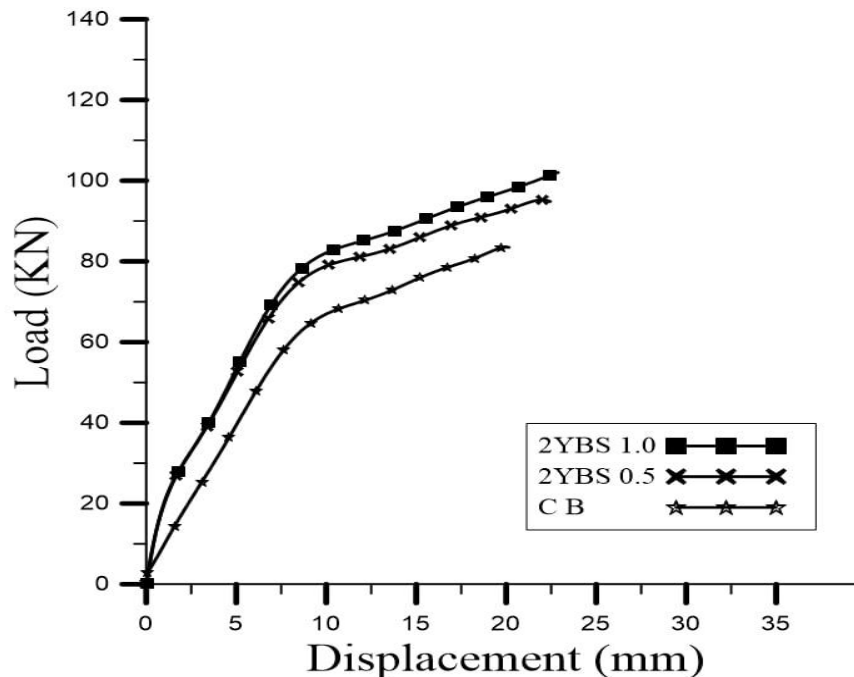


Figure 4-14: SFRC load versus deflection -Group 2



a) Failure of the beam 2YBS 0.5 by delamination problem



b) Failure of the beam 2YBS 1.0 by debonding problem

Figure 4-15: Failure modes (SFRC)concrete a): Beam 2YBS 0.5 b): Beam 2YBS 1.0

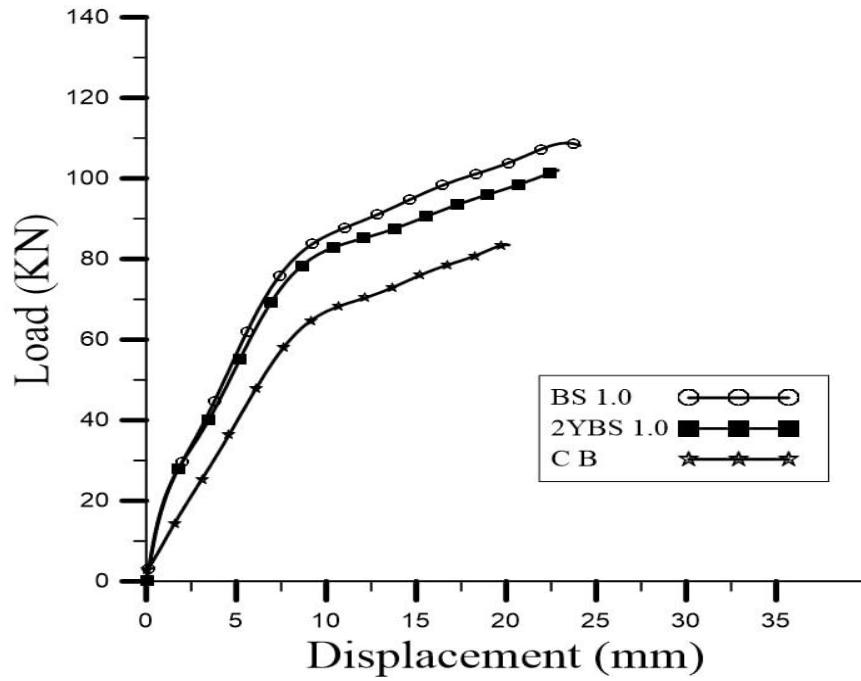


Figure 4-16: SFRC 1% load versus deflection - compared Group 2 with Group 1

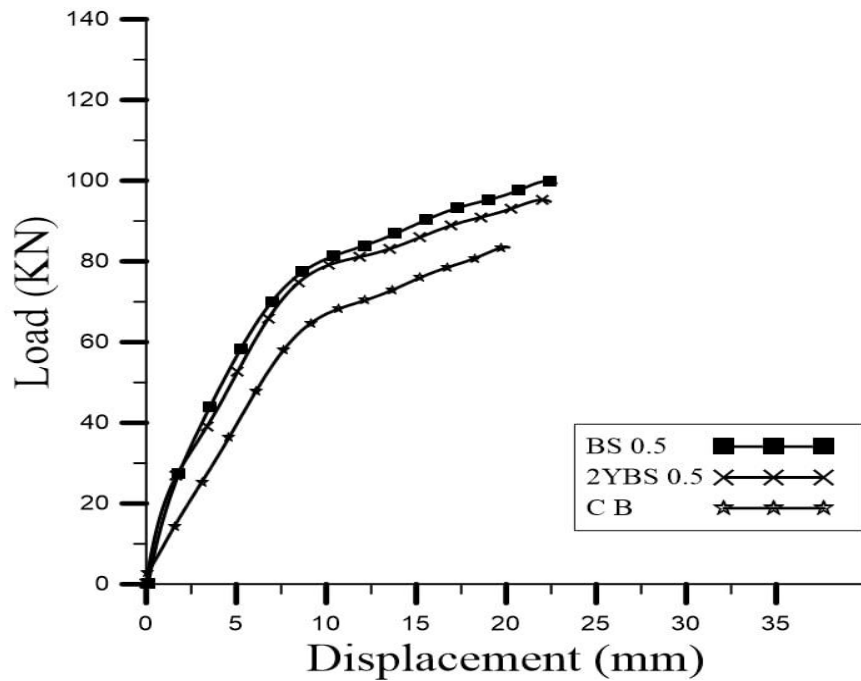


Figure 4-17: SFRC 0.5% load versus deflection - compared Group 2 with Group 1

4.5.2.2 Effect of an SFRC-PVA on the Beams that were Cast in Two Batches

The mean-range deviation was measured for both the control and containing beam 2YSFRC-2YPVA. It was found that the beams deflection for 2YBSPV 0.5.2.0, 2YBSPV 0.5.1.2, 2YBSPV 1.0.2.0 and 2YBSPV 1.0.1.2, at final load was higher than the control beam deflection (CB) by 16.43%, 19.21%, 24.42% and 27.84% respectively. The final beam load for (2YBSPV 0.5.2.0, 2YBSPV 0.5.1.2, 2YBSPV 1.0.2.0 and 2YBSPV 1.0.1.2) was 30.09%, 35.93%, 37.64% and 47.33% greater, respectively, than the control (CB) beam load, as shown in Figures 4-18 and 4-19. The failure of the beams 2YBSPV 1.0.1.2, 2YBSPV 1.0.2.0, and 2YBSPV 0.5.1.2, by debonding problem and 2YBSPV 0.5.2.0 by cover delamination problem and showed a higher loading than the control beam (C.B) Figure 4-20.

When comparing SFRC-PVA concrete with 2YSFRC-2YPVA concrete, it was noticed that the first group BSPV 0.5.2.0, BSPV 0.5.1.2, BSPV 1.0.2.0 and BSPV 1.0.1.2 had a deviation higher than the second group 2YBSPV 0.5.2.0, 2YBSPV 0.5.1.2, 2YBSPV 1.0.2.0 and 2YBSPV 1.0.1.2 by 4.46%, 3.37%, 4.96% and 6.3%, respectively, and a higher maximum load by 4.57%, 3.95%, 8.28% and 6.92%, respectively, as shown in Figures, 4-21, 4-22, 4-23 and 4-24.

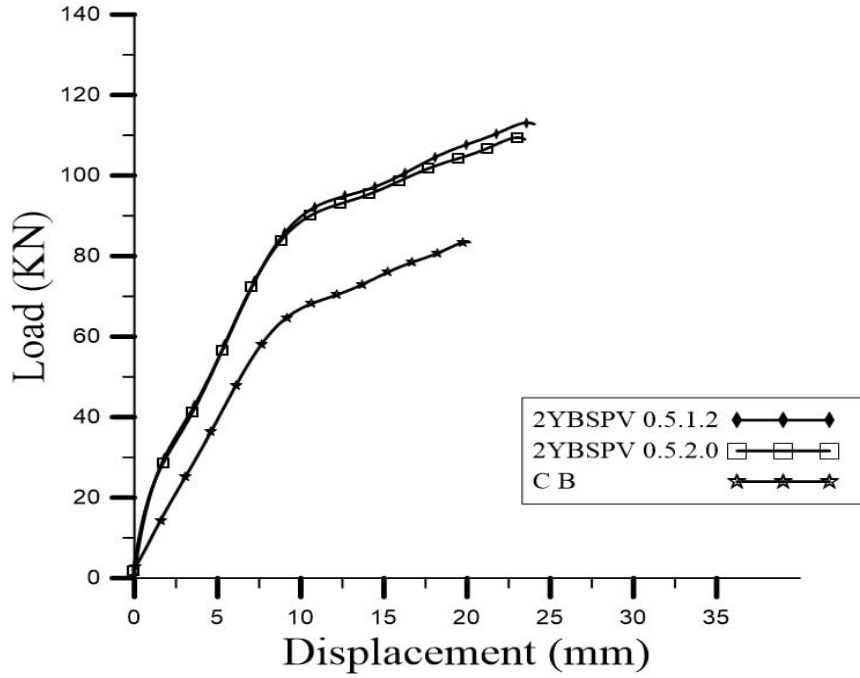


Figure 4-18: load versus deflection (2YBS 0.5% -2Y PV 1.2 , 2.0%) with (CB)

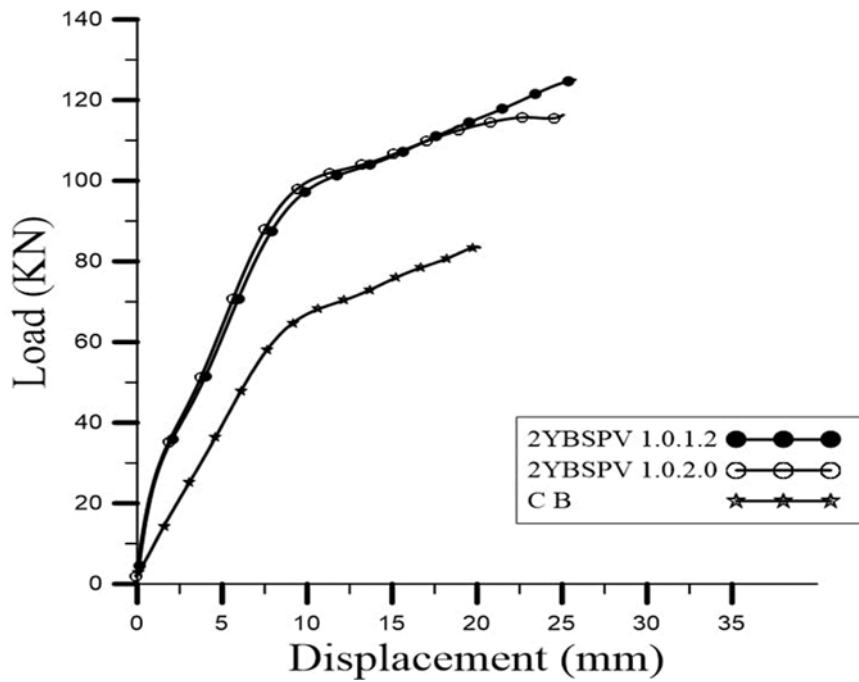
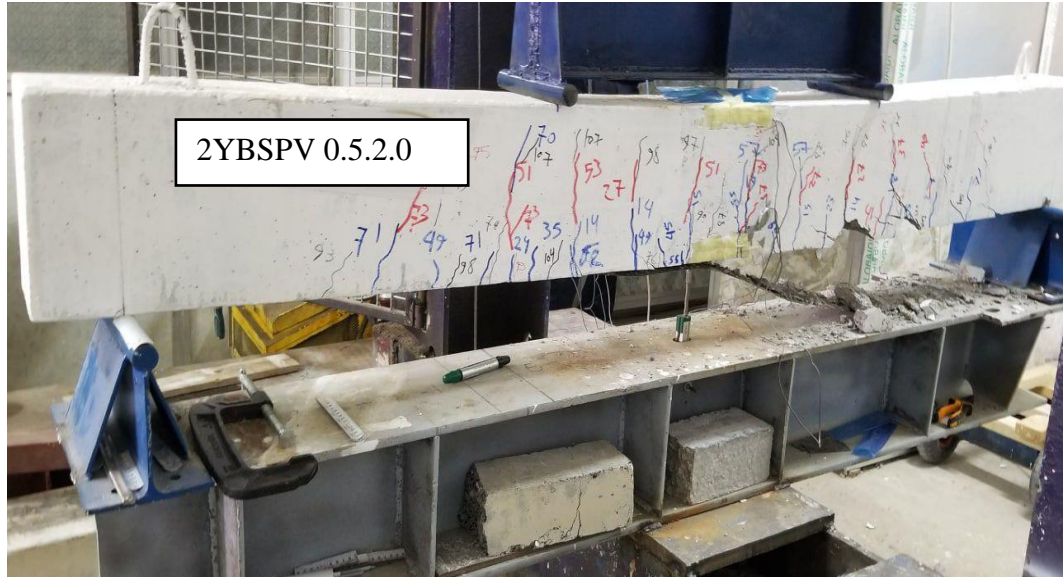


Figure 4-19: load versus deflection (2YBS 1.0% -2Y PV 1.2 , 2.0%) with (CB)



*a) Failure of the beam 2YBSPV 0.5.2.0
by delamination problem*



*b) Failure of the beam 2YBSPV 1.0.2.0
by debonding problem*



*c) Failure of the beam 2YBSPV 1.0.1.2
by debonding problem*



*d) Failure of the beam 2YBSPV 0.5.1.2
by debonding problem*

Figure 4-20: The failure of the beams 2YSFRC-2YPVA

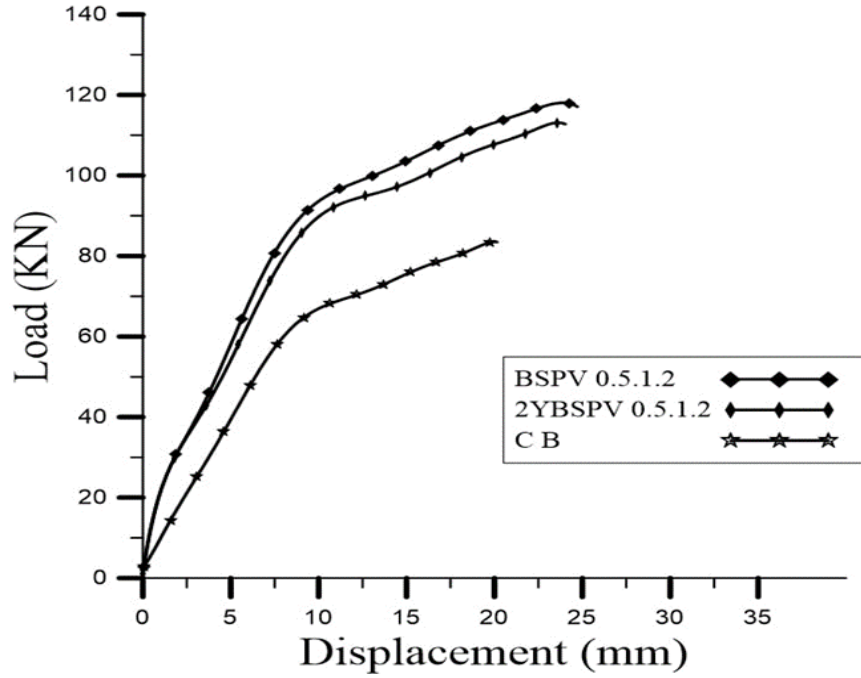


Figure 4-21: load versus deflection (2YBS 0.5.1.2 - BSPV 0.5.1.2) with (CB)

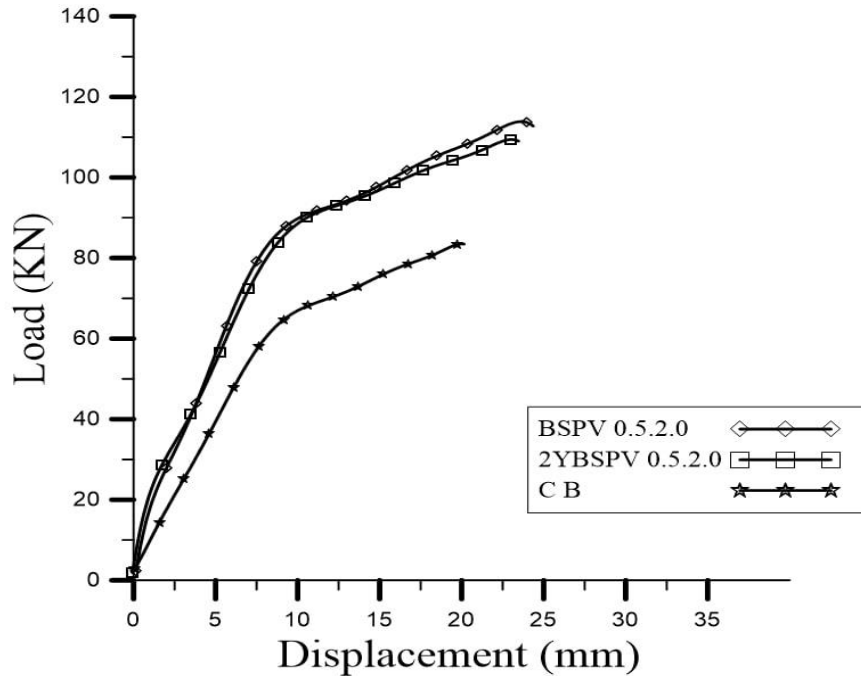


Figure 4-22: load versus deflection (2YBS 0.5.2.0 - BSPV 0.5.2.0) with (CB)

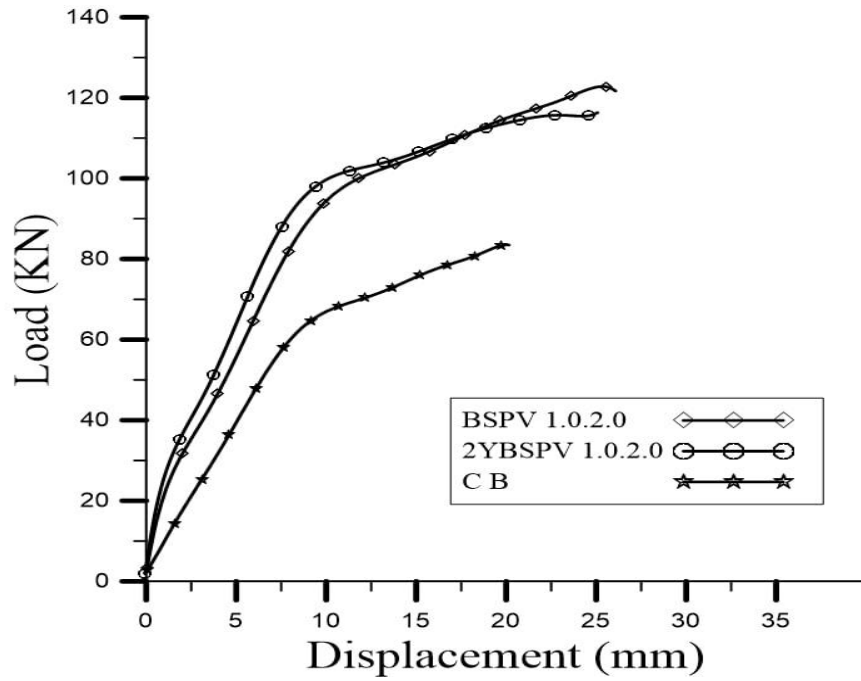


Figure 4-23: load versus deflection (2YBS 1.0.2.0- BSPV 1.0.2.0) with (CB)

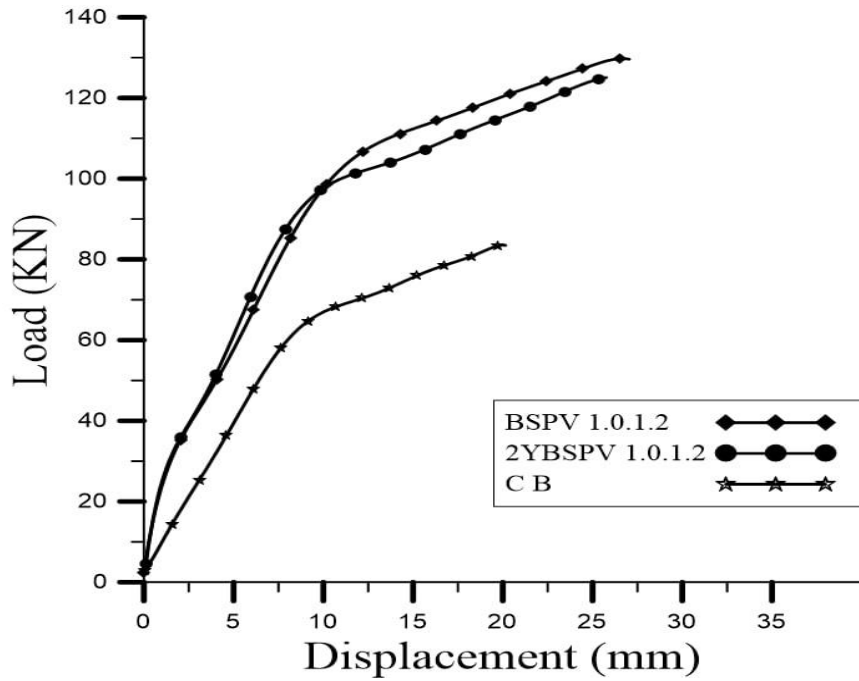


Figure 4-24: load versus deflection (2YBS 1.0.1.2 - BSPV 1.0.1.2) with (CB)

4.6 Crack Patterns and Failure Modes

Cracks first appeared in the C.B beam after the concrete's tensile capacity had been depleted. All beams in this group and the second group (Group 1 and Group 2) failed due to bending failure at increasing deflection with constant load. Several cracks appeared when the load was applied to the beam samples. Curved and diagonal cracks were observed in the control beam (C.B) during the early stages of crack loading, which began at the lower face of the beam in the middle of the span and progressed to the top of the beam as the applied load increased. Peeling failure occurred because the cracked concrete cover could not transmit the force from the CFRP. It is clear that varying the steel fiber content significantly impacted the bonding efficiency between the CFRP sheet and the SFRC beam. Because the BS 0.5 beam had low fiber content, after the CFRP sheet was ruptured, complete separation between the CFRP sheet and the beam was observed. This was due to the relatively low fiber content used in this beam. The fiber content increased to 1% as the BS1 beam demonstrated improved bonding as local delamination developed near the middle of the beam. SFRC concrete prevented substrate beams from cracking by beams BS0.5, BS1.0 by about 23.53% and 35.29%, respectively, as compared to the control beam C.B. Additionally, it could be observed that the combined effect of both SFRC - PVA showed more delay for crack appearance as exhibited by beams BSPV 0.5.2.0, BSPV 0.5.1.2, BSPV 0.5.2.0, BSPV 0.5.1.2, BSPV 1.0.2.0 and BSPV 1.0.1.2, by 35.29%,47.06%,52.94% and 70.59%, respectively. The CFRP slab was ruptured near the middle of the girder span, along with some concrete covering. It showed a greater delay in cracking, as shown in BS 0.5 and BS 1 beams. In addition, the high fiber content delayed the onset of cracks. The results also showed an improvement in the bonding area and crack appearance

by 17.65%, and 11.76% when adding 1.2 and 2% PVA due to increased tensile strength in the tension region. The peeling stress is spread over a wider area under the shaped beam. In the second group, the cracks were larger, and their appearance time was faster than in the first group because of the strength difference between the two previously described layers and the presence of a link between the two layers by their casting in two batches. Also, in the second group, at the final loading stage, additional cracks developed from the top surface in the middle of the beam due to the concrete being exposed to high compressive stress compared to the normal concrete layer (Figure 4-25). The cracking loads of the 2YBSPV 0.5.2.0, 2YBSPV 0.5.1.2, 2YBSPV 1.0.2.0, 2YBSPV 1.0.1.2, 2YBS1.0, 2YBS0.5, 2YBPV1.2 and 2YBPV2, beams in this group were delayed by 29.41%, 35.29%, 52.94%, 58.82%, 23.53%, 11.76%, 5.88% and 5.88%, compared to the control beams, respectively, recorded in SFRC - PVA and for all beams are shown in Table 4-4 for the first group and Table 4-5 for the second group.



a): Crack Patterns and Failure Modes



b): The peeling stress is spread over a wider area under the surface beam



c): Final loading stage, additional cracks developed from the top surface in the middle of the beam

Figure 4.25: Second group at the final loading stage

Chapter Five: Conclusions and Recommendations

Chapter Five: Conclusions and Recommendations

5.1 Introduction

Three flexural failure patterns plate-end interfacial debonding, concrete cover separation, and FRP rupture were seen in the tested specimens. The experiments demonstrated that the FRP rupture caused the BSPV 1.0.1.2 specimen to fail (Figure 4-9 a). In these specimens' flexural cracks appeared during the tests but they did not cause debonding of FRP sheets. C.B, BS 0.5, BPV 2.0, 2YBS 0.5, 2YBPV 1.2, 2YBPV 2.0, and 2YBSPV 0.5.2.0 specimens failed due to concrete cover separation. In these specimens, cracks began at the end of the FRP reinforcement and propagated diagonally inwards to the internal shear stirrups and then spread along the horizontal direction which caused interception of concrete cover. The FRP interface debonding caused other specimens to fail, as shown in Figure 4.25 b. The FRP sheet was detached from the beam substrate in this failure mode as a result of cracks that began at the FRP sheet's end and spread inward through the FRP and concrete interface.

5.2 Conclusions

1- The compressive strength of the concrete cube (f_c') and the tensile strength of the concrete cylinder (f_t) increases when adding 1.2% of PVA solution and 1% of steel fibers to a maximum of 65.31% and 73.79 %, respectively, compared to the control concrete.

2- The resistance to bending loads in the beams was improved by a maximum of 54.25 % in the first group beams (cast in one batch). While in the second group, the maximum increase was 47.33% when adding 1.2% of PVA solution and 1% of steel fibers.

3- The difference in the maximum load at failure for the first group of beams that were cast at once is higher than that of the beams cast in two batches. The largest difference in the maximum load is 6.92%, so this material can be added to the area around the rebar for the beams (2Y), which is more economical.

4- The cracks appeared from the bottom of the beams in almost symmetrical shapes and directions for both groups when the load applied to the beams increased. The cracks' width and length increased towards the beam's depth, causing a void between the carbon fibers and the beam and thus separation accrued.

5- PVA and SFRC concrete improve beam stiffness reduce beam deformation and number of cracks and crack widths, this type of concrete cause these cracks to spread at longer distances on the front face of the beam.

6- Increasing the percentage of steel fibers in the concrete mix from 0.5% to 1% led to an increase in the maximum load in the first and second groups by 10.91 % and 8.33%, respectively.

7- The maximum load of the bundles upon failure decreased by increasing the percentage of the PVA solution from 1.2% to 2% in the first and second groups by 4.5% and 5.39%, respectively, due to the formation of voids during mixing.

8- Beams transform sudden delamination (brittle) failure to flexural-cracks induced delamination (ductile) failure of laminate, which is advantageous in a seismically prone zone.

9- In this study, the optimum ratio was 1.2% PVA with 1% steel fiber which gave the maximum beam load at failure in both the first and second.

5.3 Future Work and Suggestions

1- Use percentages of steel fibers higher than 1% with percentages of PVA solution less than 2% to see the effect.

2- Study the effect of using other types of strengthening for PVA and SFRC concrete beams, such as near surface-mounted FRP bars.

3- Study the effect of using more than one layer of carbon fibers (CFRP) on PVA and SFRC beams.

4- SFRC-PVA concrete can be used in essential structures with high loads, such as airports, multi-story buildings, bridges, etc.

References

1. Hamid Saadatmanesh, Associate, and' Mohammad R. Ehsani, "RC BEAMS STRENGTHENED WITH GFRP PLATES. I: EXPERIMENTAL STUDY," *Manager*, vol. 117, no. 11, pp. 3417–3433, 1992.
2. Marco Arduini, and Antonio Nann, "BEHAVIOR OF PRECRACKED RC BEAMS STRENGTHENED WITH CARBON FRP SHEETS," vol. 1, no. May, pp. 63–70, 1997.
3. Minoo Panahi, Seyed Alireza Zareei, Ardavan Izadi "Flexural strengthening of reinforced concrete beams through externally bonded FRP sheets and near surface mounted FRP bars," *Construction Materials*, June, vol. 15,2021.
4. Jawad Talib Aboudi, "Ultimate Strength Capacity of R. C Space Frames Strengthened by FRP," no. May, 2008.
5. Jian Chen, "Behavior of structural concrete members strengthened by composite fabrics," *Public Health*, p. 125, 2005.
6. M. Paja and T. Ponikiewski, "Flexural behavior of self-compacting concrete reinforced with different types of steel fibers," *Construction and Building Materials*, vol. 47, pp. 397–408, 2013, doi: 10.1016/j.conbuildmat.2013.05.072.
7. H. Nordin, *Fibre reinforced polymers in civil engineering*. Licentiate thesis, pp. 143, OAI: DiVA.org: ltu-17561, 2003.
8. A. C. I. Committee, "Guide for the Design and Construction of Externally Bonded FRP Systems", American Concrete Institute, July 2008

9. O. Buyukozturk, O. Gunes, and E. Karaca, “Characterization and Modeling of Debonding in Rc Beams Strengthened With Frp Composites,” *Proc. 15th ASCE Eng. Mech. Conf.*, pp. 1–8, 2002.
10. H. M. Afefy, N. Kassem, and M. Hussein, “Enhancement of flexural behaviour of CFRP-strengthened reinforced concrete beams using engineered cementitious composites transition layer,” *Struct. Infrastruct. Eng.*, vol. 11, no. 8, pp. 1042–1053, 2015, doi: 10.1080/15732479.2014.930497.
11. Q. Wang, H. Zhu, B. Zhang, Y. Tong, F. Teng, and W. Su, “Anchorage systems for reinforced concrete structures strengthened with fiber-reinforced polymer composites: State-of-the-art review,” *J. Reinf. Plast. Compos.*, vol. 39, no. 9–10, pp. 327–344, 2020, doi: 10.1177/0731684420905010.
12. Robert C. Creese R. C. Creese, “Polymer Composites II: Composites Applications in Infrastructure Renewal and Economic Development,” p. 256, CRC Press, 2001
13. Dejian Shen, C. Wen, P. Zhu, Y. Wu, and J. Yuan “Influence of Barchip fiber on early-age autogenous shrinkage of high strength concrete,” *J. Construction and Building Materials*, vol. 256, pp. 119-223, 2020, doi: 10.1016/j.conbuildmat.2020.119223.
14. K. Benzarti, F. Freddi, and M. Frémond, “A damage model to predict the durability of bonded assemblies. Part I: Debonding behavior of FRP strengthened concrete structures,” *Constr. Build. Mater.*, vol. 25, no. 2, pp. 547–555, 2011, doi: 10.1016/j.conbuildmat.2009.10.018.
15. A. Khalifa, W. J. Gold, A. Nanni, and A. A. M.I., “Contribution of Externally Bonded FRP to Shear Capacity of RC Flexural Members,” *J.*

- Compos. Constr., vol. 2, no. 4, pp. 195–202, 1998, doi: 10.1061/(asce)1090-0268(1998)2:4(195).
16. O. Buyukozturk, O. Gunes, and E. Karaca, “Progress on understanding debonding problems in reinforced concrete and steel members strengthened using FRP composites,” *Constr. Build. Mater.*, vol. 18, no. 1, pp. 9–19, 2004, doi: 10.1016/S0950-0618(03)00094-1.
 17. P. Investigations, “Concrete Repair with CFRP,” *Concr. Int.*, no. May, pp. 45–52, 2004.
 18. T. C. Triantafillou and N. Plevris, “Strengthening of RC beams with epoxy-bonded fibre-composite materials,” *Mater. Struct.*, vol. 25, no. 4, pp. 201–211, 1992, doi: 10.1007/BF02473064.
 19. W. P. Boshoff, “Time-Dependant Behaviour of Engineered Cement-Based Composites,” vol. Ph.D. Thesis, no. March, p. 182, 2007, <http://hdl.handle.net/10019.1/1249>.
 20. C. C. Thong, D. C. L. Teo, and C. K. Ng, “Application of polyvinyl alcohol (PVA) in cement-based composite materials: A review of its engineering properties and microstructure behavior,” *Constr. Build. Mater.*, vol. 107, pp. 172–180, 2016, doi: 10.1016/j.conbuildmat.2015.12.188.
 21. M. Drabik, S. C. Mojumdar, and R. C. T. Slade, “Prospects of novel macro-defect-free cements for the new millennium,” *J.Ceram. - Silikaty*, vol. 46, no. 2, pp. 68–73, 2002.
 22. J. A. Lewis and M. A. Boyer, “Effects of an organotitanate cross-linking additive on the processing and properties of macro-defect-free cement,” *Adv. Cem. Based Mater.*, vol. 2, no. 1, pp. 2–7, 1995, doi: 10.1016/1065-7355(95)90033-0.

23. J. H. Kim and R. E. Robertson, "Prevention of air void formation in polymer-modified cement mortar by pre-wetting," *Cem. Concr. Res.*, vol. 27, no. 2, pp. 171–176, 1997, doi: 10.1016/S0008-8846(97)00001-X.
24. S. Wang and V. Li, "Tailoring of pre-existing flaws in ECC matrix for strain hardening," *Mechanics of Concrete Structures*, pp. 1005–1012, 2004.
25. J. F. Chen and J. G. Teng, "Shear capacity of FRP-strengthened RC beams: FRP debonding," *Constr. Build. Mater.*, vol. 17, no. 1, pp. 27–41, 2003, doi: 10.1016/S0950-0618(02)00091-0.
26. T. Wongtanakitcharoen and A. E. Naaman, "Unrestrained early age shrinkage of concrete with polypropylene, PVA, and carbon fibers," *Mater. Struct. Constr.*, vol. 40, no. 3, pp. 289–300, 2007, doi: 10.1617/s11527-006-9106-z.
27. Y. Singh, S. Singh, and H. Singh, "Effect of Steel Fibers on the Sorptivity of Concrete," *Lect. Notes Mech. Eng.*, vol. 9, no. I, pp. 479–491, 2021, doi: 10.1007/978-981-15-4779-9_32.
28. F. Köksal, F. Altun, I. Yiğit, and Y. Şahin, "Combined effect of silica fume and steel fiber on the mechanical properties of high strength concretes," *Constr. Build. Mater.*, vol. 22, no. 8, pp. 1874–1880, 2008, doi: 10.1016/j.conbuildmat.2007.04.017.
29. M. Nili and V. Afroughsabet, "Combined effect of silica fume and steel fibers on the impact resistance and mechanical properties of concrete," *Int. J. Impact Eng.*, vol. 37, no. 8, pp. 879–886, 2010, doi: 10.1016/j.ijimpeng.2010.03.004.
30. B. Hearing, "Delamination in Reinforced Concrete Retrofitted with Fiber Reinforced Plastics," Thesis, 2000.

31. R. Strains *et al.*, “Annex 1: Case of study ‘Repair of bridges using Fiber Reinforced Polymers (FRP),’” pp. 1–13.
32. M. Al-Farttoosi, “Impact Behaviour of Reinforced Concrete Beams Strengthened or Repaired with Carbon Fibre Reinforced Polymer (CFRP),” 2016, <https://pearl.plymouth.ac.uk/handle/10026.1/6701>.
33. A. Carolin, *Carbon Fibre Reinforced Polymers for Strengthening of Structural Elements*, vol. 1992, no. 10. 2003.
34. F. Ceroni, “Experimental performances of RC beams strengthened with FRP materials,” *Constr. Build. Mater.*, vol. 24, no. 9, pp. 1547–1559, 2010, doi: 10.1016/j.conbuildmat.2010.03.008.
35. Y. J. Kim and P. J. Heffernan, “Fatigue Behavior of Externally Strengthened Concrete Beams with Fiber-Reinforced Polymers: State of the Art,” *J. Compos. Constr.*, vol. 12, no. 3, pp. 246–256, 2008, doi: 10.1061/(asce)1090-0268(2008)12:3(246).
36. A. Khalifa and A. Nanni, “Improving shear capacity of existing RC T-section beams using CFRP composites,” *Cem. Concr. Compos.*, vol. 22, no. 3, pp. 165–174, 2000, doi: 10.1016/S0958-9465(99)00051-7.
37. C. M. Davidson, A. L. Duncan, D. Littlejohn, A. M. Ure, and L. M. Garden, “A critical evaluation of the three-stage BCR sequential extraction procedure to assess the potential mobility and toxicity of heavy metals in industrially-contaminated land,” *Anal. Chim. Acta*, vol. 363, no. 1, pp. 45–55, 1998, doi: 10.1016/S0003-2670(98)00057-9.
38. F. Al-Mahmoud, A. Castel, R. François, and C. Tourneur, “RC beams strengthened with NSM CFRP rods and modeling of peeling-off failure,” *Compos. Struct.*, vol. 92, no. 8, pp. 1920–1930, 2010, doi: 10.1016/j.compstruct.2010.01.002.

39. L. De Lorenzis, B. Miller, and A. Nanni, "Bond of fiber-reinforced polymer laminates to concrete," *ACI Mater. J.*, vol. 98, no. 3, pp. 256–264, 2001, doi: 10.14359/10281.
40. L. De Lorenzis and J. G. Teng, "Near-surface mounted FRP reinforcement: An emerging technique for strengthening structures," *Compos. Part B Eng.*, vol. 38, no. 2, pp. 119–143, 2007, doi: 10.1016/j.compositesb.2006.08.003.
41. A. Pimanmas, "Strengthening R/C beams with opening by externally installed FRP rods: Behavior and analysis," *Compos. Struct.*, vol. 92, no. 8, pp. 1957–1976, 2010, doi: 10.1016/j.compstruct.2009.11.031.
42. T. C. Triantafillou and N. Plevris, "Strengthening of RC beams with epoxy-bonded fibre-composite materials," *Mater. Struct.*, vol. 25, no. 4, pp. 201–211, 1992, doi: 10.1007/BF02473064.
43. E. Y. Sayed-ahmed, A. H. Riad, and N. G. Shrive, "bonded carbon fibre reinforced polymer strips or external post-tensioning Flexural strengthening of precast reinforced concrete bridge girders using bonded carbon fibre reinforced polymer strips or external post-tensioning," no. June, 2004, doi: 10.1139/104-005.
44. C. Czaderski and U. Meier, "EBR strengthening technique for concrete, long-term behaviour and historical survey," *Polymers (Basel)*, vol. 10, no. 1, 2018, doi: 10.3390/polym10010077.
45. U. Meier, "Strengthening of structures using carbon fibre/epoxy composites," *Constr. Build. Mater.*, vol. 9, no. 6, pp. 341–351, 1995, doi: 10.1016/0950-0618(95)00071-2.
46. J. Yin and Z. S. Wu, "Structural performances of short steel-fiber reinforced concrete beams with externally bonded FRP sheets," *Constr.*

- Build. Mater.*, vol. 17, no. 6–7, pp. 463–470, 2003, doi: 10.1016/S0950-0618(03)00044-8.
47. M. R. Esfahani, M. R. Kianoush, and A. R. Tajari, “Flexural behaviour of reinforced concrete beams strengthened by CFRP sheets,” *Eng. Struct.*, vol. 29, no. 10, pp. 2428–2444, 2007, doi: <https://doi.org/10.1016/j.engstruct.2006.12.008>.
48. E. Benvenuti and N. Orlando, “Failure of FRP-strengthened SFRC beams through an effective mechanism-based regularized XFEM framework,” *Compos. Struct.*, vol. 172, pp. 345–358, 2017, doi: 10.1016/j.compstruct.2017.02.099.
49. H. Najm, A. E. Naaman, T. J. Chu, and R. E. Robertson, “Effects of poly(vinyl alcohol) on fiber cement interfaces. Part I: Bond stress-slip response,” *Adv. Cem. Based Mater.*, vol. 1, no. 3, pp. 115–121, 1994, doi: 10.1016/1065-7355(94)90042-6.
50. T. J. Chu, R. E. Robertson, H. Najm, and A. E. Naaman, “Effects of poly(vinyl alcohol) on fiber cement interfaces. Part II: Microstructures,” *Adv. Cem. Based Mater.*, vol. 1, no. 3, pp. 122–130, 1994, doi: 10.1016/1065-7355(94)90043-4.
51. ACI committee 318, *Building Code Requirements for Structural Concrete and Commentary (ACI 318M-11)*. 2011.
52. ASTM.C33, “Standard specification for concrete aggregates,” *Philadelphia, PA Am. Soc. Test. Mater.*, 2003.
53. A. Drews, “Standard Test Method for Split Tensile Strength,” *Man. Hydrocarb. Anal. 6th Ed.*, pp. 545-545–3, 2008, doi: 10.1520/C0496.
54. ASTM, “Standard specification for deformed and plain billet-steel bars for concrete reinforcement,” 2000.

55. P. D. Sheet, S. Viscocrete, S. Viscocrete, S. Viscocrete, S. Viscocrete, and P. Data, “Sika ViscoCrete ® F180G,” pp. 3–5, 2018.
56. ASTM. C494, “597: Standard Test Method for Pulse Velocity through Concrete. Annual Book of ASTM Standards.” West Conshohocken, Pa: ASTM, 1999.
57. 143M. ASTM, “Standard test method for slump of hydraulic-cement concrete,” *ASTM Int. West Conshohocken, PA*, 2012.
58. BS 1881-125: “BSI Standards Publication Testing concrete — Part 125: Methods for mixing and sampling fresh concrete in the laboratory,” *Br. Stand.*, no. April, 2013.
59. ASTM C469-11, “Standard Test Method for Splitting Tensile Strength of Cylindrical Concrete Specimens,” *Man. Hydrocarb. Anal. 6th Ed.*, vol. i, pp. 545-545–3, 2008, doi: 10.1520/C0496.
60. O. Gencel, W. Brostow, T. Datashvili, and M. Thedford, “Workability and mechanical performance of steel fiber-reinforced self-compacting concrete with fly ash,” *Compos. Interfaces*, vol. 18, no. 2, pp. 169–184, 2011, doi: 10.1163/092764411X567567.
61. A. Allahverdi, K. Kianpur, and M. R. Moghbeli, “Effect of polyvinyl alcohol on flexural strength and some important physical properties of Portland cement paste,” *Iran. J. Mater. Sci. Eng.*, vol. 7, no. 1, pp. 1–6, 2010.
62. S. Syed Ibrahim, S. Kandasamy, S. Pradeepkumar, and R. Subash Chandra Bose, “Effect of discrete steel fibres on strength and ductility of FRP laminated RC beams,” *Ain Shams Eng. J.*, vol. 12, no. 2, pp. 1329–1337, 2021, doi: 10.1016/j.asej.2020.10.005.

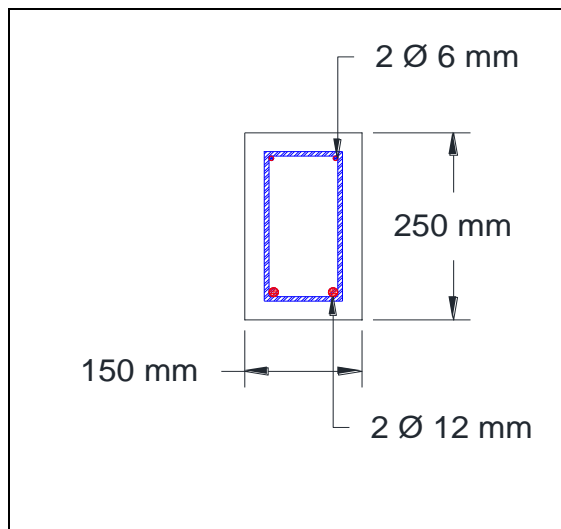
Appendices

Appendix A

Design of control Beam

The beam's dimensions are constrained for experimental purposes.

(Prototype model) to depth 0.250 m, width 0.150 m, and 2.15 m in length. The material properties are $f_y = 420 \text{ MPa}$, $f_c' = 30 \text{ MPa}$ for steel and concrete.



Cross section area of control beam

Design of Beams

were

f_c' = compressive strength, and

A_g = gross area of the cross-section.

Cover = 20 mm

$$d = \text{depth} - \text{cover} - \frac{db}{2} - d \text{ stirrup}$$

$$d = 250 - 20 - \frac{12}{2} - 6 = 218 \text{ mm}$$

$$A_s = 2 * \frac{\pi(144)}{4} = 226.2 \text{ mm}^2$$

$$\rho = \frac{A_s}{b*d} = \frac{226.2}{150*218} = 0.006917$$

$$\rho_{\max} = \frac{f_c'}{f_y} * 0.85 * \beta + \frac{\epsilon_{cu}}{\epsilon_{cu} + 0.004}$$

$$\beta = 0.85 - \frac{30-28}{7} * 0.05 = 0.84$$

$$\rho_{\max} = 0.85 * 0.84 * \frac{30}{420} * \frac{0.003}{0.003 + 0.004} = 0.0216$$

$$\rho_{\min} = 0.25 * \frac{\sqrt{f_c'}}{f_y} = 0.00326$$

$$\rho_{\min} < \rho < \rho_{\max} \quad \text{O.K.}$$

$$M_u = p * s + \frac{w * l^2}{8}$$

$$M_n = A_s * f_y * (d - \frac{a}{2})$$

$$a = \beta * c$$

$$T = c$$

$$A_s * f_y = 0.85 * f_c' * b * a$$

$$a = \frac{A_s * f_y}{0.85 * f_c' * b} = \frac{226.2 * 463.1}{0.85 * 34.6 * 150} = 23.72 \text{ mm}$$

$$c = \frac{a}{\beta} = 28.24 \text{ mm}$$

$$\frac{\epsilon_{cu}}{c} = \frac{\epsilon_t}{d - c}$$

$$\frac{0.003}{30} = \frac{\epsilon_t}{218 - 30} = 0.0188 > 0.005 \rightarrow \phi = 0.9$$

$$M_n = 226.2 * 463.1 * (218 - \frac{23.72}{2}) * 10^6$$

$$M_n = 21.57 \text{ kN.m}$$

$$M_n = p \cdot a$$

$$21.57 = p \cdot 0.71$$

$$P = 30.38 \text{ kN}$$

$$2p = 60.76 \text{ kN}$$

$$V_{ud} = 0.69 \cdot \frac{2}{2} + 23.77 = 24.46 \text{ kN}$$

$$\phi V_c = 0.75 \cdot \left(\frac{\sqrt{f_c'}}{6} \right) bd = 22.38 \text{ kN}$$

$$V_s = \frac{V_{ud} - \phi V_c}{\phi} = 2.77 \text{ kN}$$

$$V_s < 4 \cdot V_c = 89.52 \text{ kN} \rightarrow \text{O.K.}$$

$$2.77 < 2 \cdot V_c = 44.76 \text{ kN}$$

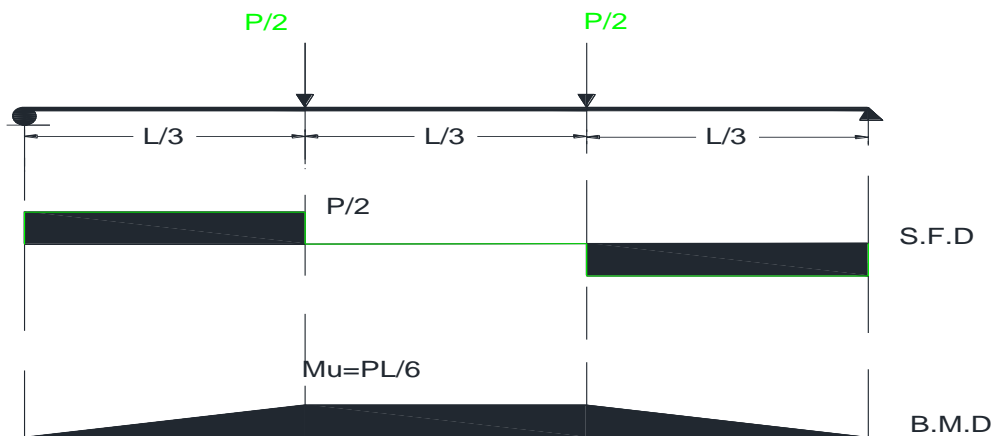
Use ϕ 6 mm

$$S_{\max} = \frac{d}{2} = 109 \text{ mm}$$

$$\text{OR } S_{\max} = \frac{A_v \cdot f_y}{b_w} = 474.9 \text{ mm}$$

$$\text{OR } S_{\max} = \frac{A_s \cdot f_y}{\sqrt{f_c'} \cdot b_w} = 462 \text{ mm}$$

$$S_{\text{req.}} = \frac{A_v \cdot f_y \cdot d}{V_s} = 186.8 \text{ mm}$$



Bending moment and shear force diagram

الخلاصة

تستخدم ألواح البوليمر المقوى بألياف الكربون (CFRP) لتحسين خصائص الخرسانة في المكونات الهيكلية مثل المباني والجسور. يُنظر إلى هذه التقنية المركبة بشكل شائع حيثما تكون نسبة القوة إلى الوزن والصلابة مطلوبة. ومع ذلك ، فإن إحدى المشكلات المهمة في هذا النظام هي مشكلة التفريغ. عند مستوى تحميل معين ، تبدأ صفائح البلاستيك المقوى بألياف الكربون في الفصل من العتب الخرسانية ، مما يؤدي إلى فشل سابق لأوانه. نتيجة لذلك ، يهدف هذا البحث التجريبي إلى التحكم في التفريغ باستخدام كحول بولي فينيل (PVA) وألياف الصلب (SFRC) بنسب وترتيبات وتقنيات مختلفة. اعتمد البرنامج العملي للدراسة المقدمة على صب (17) عتب مستطيلة من الخرسانة المسلحة بأبعاد مقطعية (250 * 150) ملم وطول (2150) ملم تم تقويتها بألواح CFRP. كان الأول عبارة عن عتب تحكم بدون PVA أو SFRC. تم تقسيم العينات الستة عشر المتبقية إلى مجموعتين. تتكون المجموعة الأولى من ثماني عتاب تم صبها بالكامل بمواد PVA و SFRC. تتكون المجموعة الثانية من ثماني حزم أخرى تم صبها باستخدام PVA و SFRC من الطبقة السفلية للحزمة حتى ارتفاع 52 مم. أوضحت النتائج أن استخدام 1.2% من PVA و 1% من الألياف الفولاذية زاد من القوة القصوى وانحراف منتصف المدى لكلا المجموعتين مقارنة بعتب التحكم. هناك حاجة إلى قيم محددة ، حيث كانت الزيادة القصوى في حمل فشل العتب 54.3% و 47.3% ، وكانت أكبر زيادة في إزاحة منتصف العتب 34.14% و 27.84% للمجموعتين الأولى والثانية على التوالي. يتمثل دور الطبقة المقترحة (PVA / SFRC) في التحكم في تكسير الخرسانة وحجز أو حتى تجنب التقليل المبكر لألواح البلاستيك المقوى بألياف الكربون المقوى. نظرًا لأن قدرة الطبقة (PVA / SFRC) على إظهار سلوك تصلب الإجهاد يتم تحديدها بشكل أساسي من خلال النسبة الحجمية للألياف المستخدمة ، فإن نسبتين مختلفتين من الألياف الفولاذية الحجمية (النسب الحجمية للألياف 0.5% و 1% ، على التوالي) زادت من الحد الأقصى للحمل في الأول والثانية بنسبة 10.91% و 8.33% على التوالي. شوهدت ثلاثة أنماط لفشل الانحناء - إزالة الترابط بين نهاية الصفائح ، وفصل الغطاء الخرساني ، وتمزق FRP في العينات المختبرة. أظهرت التجارب أن تمزق FRP تسبب في فشل العتب BSPV 1.0.1.2.



جمهورية العراق

وزارة التعليم العالي و البحث العلمي

جامعة كربلاء

كلية الهندسة

قسم القنطرة المدنية

اطروحة

تحسين قدرة الانحناء للعتبات الخرسانية المسلحة المعززة بالواح الكربون

مقدم لكلية الهندسة جامعة كربلاء في استيفاء جزئي لمتطلبات درجة ماجستير العلوم في الهندسة المدنية

الباحث

محمد علي عزيز

(بكالوريوس. في الهندسة المدنية -2016)

باشراف

أ.م.د. جواد طالب عبودي

أ.م.د. ايمن جميل كاظم